World Journal of Research and Review (WJRR)
ISSN:2455-3956, Volume-6, Issue-3, March 2018 Pages 38-61

North Anatolian Fault Zone, Northern Turkey: Empirical Equations and the Changes in Some Kinematic Characteristics

Mehmet UTKU

Abstract- **Monitoring the seismological development of a seismotectonic source is important to know the future behavior of the source concerned. The North Anatolian Fault Zone is one of the important seismotectonic sources in the world. The seismic moment-magnitude relations were computed according to the macroseismic and instrumental observations of 29 earthquakes with $m_{b,S} \geq 4.8$ that occurred in the North Anatolian Fault Zone in the 1909-2000 period. The relations of seismic moment for this tectonic structure according to the surface wave magnitude and according to the fault area and the change in stress drop are the other seismological characteristics addressed in this study. Depending on the other parameters within the scope of the study, the threshold magnitude value and the mean slip rate for the visible fault on the ground surface are computed as 6.2 (M_s) and 2.2 cm/year, respectively. According to the 13958 earthquakes with M ≥ 3.0 that occurred in the North Anatolian Fault Zone in the period between 11/24/0029 (29 A.D.) and 12/31/2014, the return period of a possible major earthquake to be generated by this zone is 250 years at the most. The a- and b- values which characterize the Zone are 4 and - 0.8 on an average, respectively.**

When the results in this study – obtained according to the 91-year data process and the 101-year evaluation process – are compared with the results known from the previous studies, the latest results appear more reliable both in terms of the length of the process considered and the quality of the data used. When the behavior of the seismotectonic source concerned is monitored depending on this, it is seen that some seismological characters remained stable, while some of them changed.

Index Terms - **NAFZ, Empirical equations, threshold magnitude, stress drop, seismic moment, slip rate, a- values, b- values.**

I. INTRODUCTION

The North Anatolian Fault Zone (NAFZ) is an essential tectonic structure which plays the leading role in the regional tectonics thanks to the intracontinental transform fault identity it has maintained so far [53], [52], [8]. It is an approximately 1400-km-long seismotectonic source that originates from the surroundings of Karlıova (Bingöl) in the east, continues with three branches after Niksar (Tokat), Ladik (Samsun), Kargı (Çorum), Tosya (Kastamonu) and Bolu, crosses the Marmara, and reaches the Aegean Sea. The NAFZ, which last gained currency with the August 17, 1999 (M_w=7.4) Gölcük (İzmit) earthquake and the November 12, 1999 (M_w=7.2) Düzce (Bolu) earthquake, has a branch that crosses the Gulf of İzmit via Düzce, Akyazı (Adapazarı), Sapanca (Adapazarı), Gölcük (İzmit) and Hersek (İzmit), meets the Ganos (Gaziköy, Tekirdağ) Fault to the north of the Marmara Sea, and is conveyed to the Aegean Sea. Its other branch again reaches the Ganos Fault via Geyve (Adapazarı), İznik (Bursa) and Gemlik (Bursa) routes after Bolu, in the south of the Armutlu Peninsula and by passing through the Marmara Sea almost centrally. Another branch of it progresses on land in the south of the Marmara Sea and extends to the Aegean Sea via the Biga Peninsula.

So far, many studies have been made with respect to the NAFZ [38], [37], [39], [23], [36], [17], [56], [54], [55], [7], [6], [5], [16], [27]. Mean displacement velocities of 3 cm/year or 4 cm/year and even up to 11 cm/year were found in these studies according to the data then [4], [35], [11]. Of them, a similar study which *most closely fit* the information obtained from the observation results and from the instrumental data was made by Canıtez and Ezen (1973) with 8 earthquakes with $m_b \geq 6.0$ in the 1900-1971 period, and it calculated the stress drops of 39 earthquakes by deriving statistics. Later on, the 8 earthquakes with M_s>6.0 between 1939 and 1967 were used by Ezen (1981) to estimate various relations between source parameters and magnitude. Some 7 earthquakes were common in both studies. Barka and Kadinsky-Cade (1988) investigated the segmentation of two major strike-slip fault zones in Turkey. Wells and Coppersmith (1994) compiled 421 historical earthquakes worldwide. By using 244 earthquakes selected, they developed the empirical relationships among various source parameters such as moment magnitude, surface rupture length, subsurface rupture length, downdip rupture width, rupture area, and maximum and average displacement.

Of the studies in recent years, Ambraseys and Jackson (2000) deal with the seismic activity that occurred in the Marmara Sea in the last 500 years. Accordingly, it is stated that an evident seismic activity was experienced in the Marmara Region in the 20th century; however, throughout these 500 years, only the 18th century displayed a comparative seismic activity that also had processes which did not generate earthquakes with a magnitude of 6.8 (M_s) and greater. Moreover, two regions with late Quaternary faulting are mentioned, namely the north-west of the Marmara Sea and the southern branch of the North Anatolian Fault to the east of Bursa. The same authors state that the historic earthquakes near İstanbul had magnitudes in the range

Mehmet UTKU Department of Geophysical Engineering, Faculty of Engineering, Dokuz Eylül University, TR-35160, Buca-İzmir, Turkey

6.8-7.2 (M_s) and occurred offshore and that the smaller ones occurred in the east and west of the Marmara Sea. In addition, they note that the seismicity for the last 500 years has been taking place with right-lateral displacement above 22 ± 3 mm/year, expected in the Marmara Region. Gürbüz et al. (2000) indicate the seismic gaps concerning the 1754 earthquake with an epicenter corresponding to the Gulf of İzmit and the 1766 earthquake with an epicenter corresponding to the central Marmara basin, both with a magnitude of 7.5, in the seismotectonics of the Marmara Region that they discussed on the basis of the minor earthquakes they had recorded. Furthermore, they state that the distribution of depths belonging to the seismicity in this area is shallower than 15 km. Polat et al. (2002a,b) discuss the August 17, 1999 (M_w = 7.4) Gölcük (İzmit) earthquake in terms of the change in seismicity, its aftershocks, and the regional seismotectonics. In their study, the authors emphasize that there had been no evident seismic activity before the earthquake concerned. By quoting from Barka et al. (2000), Polat et al. (2002a) state that the surface fault of the İzmit earthquake was above 150 km in the E-W direction and that the maximum displacement was measured as 5 m. In addition, they explain that the aftershocks were distributed in the upper section of the depth of the first 15 km and that 90% of them had depths between 5 and 15 km. They stress that the depth of the main shock was 15 km. Utku (2003) investigated the macroseismic and instrumental observations for 29 earthquakes with magnitudes $m_b \geq 4.8$ that occurred in the 1900-2002 period. In this study, they computed the stress drop as below 50 bars and intended to estimate the seismic character of the zone concerned from the behavior of the maximum annual magnitudes. Accordingly, the behavior curve concerned reaches the maximum point 15 years after the minimum point on average. The data period available for this evaluation based on data of almost 100 years is significant. Bayrak and Öztürk (2004) discuss the time and spatial changes of the sequences of aftershocks of the 1999 İzmit and Düzce earthquakes. Accordingly, the b- value is provided as 1.10 for the sequences of the İzmit earthquakes and as 1.16 for the sequences of the Düzce earthquakes. They emphasize that these computed values are the characteristic b- values representing the sequences of aftershocks. Furthermore, they provide the ranges of b-values as 0.8-1.5 and 0.8-1.6 for the İzmit and Düzce sequences, respectively. They state that the highest b-value is in Adapazarı-Hendek, the east of Akyazı and the western end of the rupture, whereas the lowest b- value is between Lake Sapanca and the epicenter of the main shock. Şengör et al. (2005) carried out a review study for the North Anatolian Fault Zone. Ezen and Irmak (2007) calculated the stress drop in the North Anatolian Fault Zone for 9 strong earthquakes with magnitudes $6.5 \leq M_w \leq 7.9$ that occurred in the 1939-1999 period. In their study, they found that the stress drop was 50 bars and below. Accordingly, they stated that the stress drop in the zone concerned did not depend significantly on the earthquake magnitude and that it was particularly shaped by stress accumulation and creep. Bayrak et al. (2011) discussed the evaluation in the earthquake hazard parameters by dividing the North Anatolian Fault Zone into different segments. They used the method of Kijko and Sellevoll (1989, 1992) in this study of theirs. Yucemen and Akkaya (2012) present a case study about the estimation of magnitude-frequency relationship using the Modified Maximum Likelihood method. Le Pichon et al. (2014) defined the geometry of the Southern Marmara Fault particularly on the basis of the exploration of seismic reflection profiles. Şengör et al. (2014) described the geometry of the North Anatolian Fault Zone in the Sea of Marmara in light of the multichannel seismic reflection profiles in the Sea of Marmara. Scholz (2002), Shaw and Wesnousky (2008), Senatorski (2012), Shaw (2013) and Konstantinou (2014) dealt with the mechanics and kinematics of earthquakes and the faulting process. One of the recent studies was made by Yamamoto et al. (2015). In the study, they analyzed the data recorded by three ocean bottom seismographs (OBSs) over a period of 3 months in 2014 to investigate the relationship of fault geometry to microseismicity under the western Marmara Sea in Turkey. They showed that most of the microearthquakes they identified occurred along the Marmara Fault (MMF). Their data indicate that the fault plane of the MMF is almost vertical. They identified a seismogenic zone that extends from 13 to 25 km depth through the upper and lower crust beneath the western Marmara Sea.

In this study, the seismic moment (M_0)-magnitude (m_b,M_s) and seismic moment-fault plane (A) relations and the change in stress drop ($\Delta\tau$) that occurred along the zone are examined according to the data about the earthquakes with $m_{b,s} \geq 4.8$ that occurred in the NAFZ in the 1900-2000 process. m_b and M_s denote body and surface wave magnitudes, respectively. The study also encompasses the threshold magnitude value and the total and mean displacement velocities for the visible fault along the zone concerned. As it will also be understood from the period limits addressed, the results obtained depend on the latest seismological data and constitute the latest seismological identity. Comparing the previous results with a similar scope and the present results is another stage of this study. In this way, it will be possible to monitor and examine the behavior of the seismotectonic source concerned and review its character throughout a process.

Moreover, in this study the earthquake hazard of the North Anatolian Fault Zone was investigated by using 13958 earthquakes with magnitudes 3 and greater that occurred between 29 A.D. and 12/31/2014. Figure 1 shows the epicenter distribution of the 13958 earthquakes used in this study. The data used belong to the electronic earthquake catalogue of Kandilli Observatory and Earthquake Research Institute of Boğaziçi University. The zone of deformation of the Fault has been divided into subzones of deformation considering the epicenter clusters and the tectonism of the Zone, and the results of these subzones have been thoroughly investigated comparatively. This thorough investigation has been

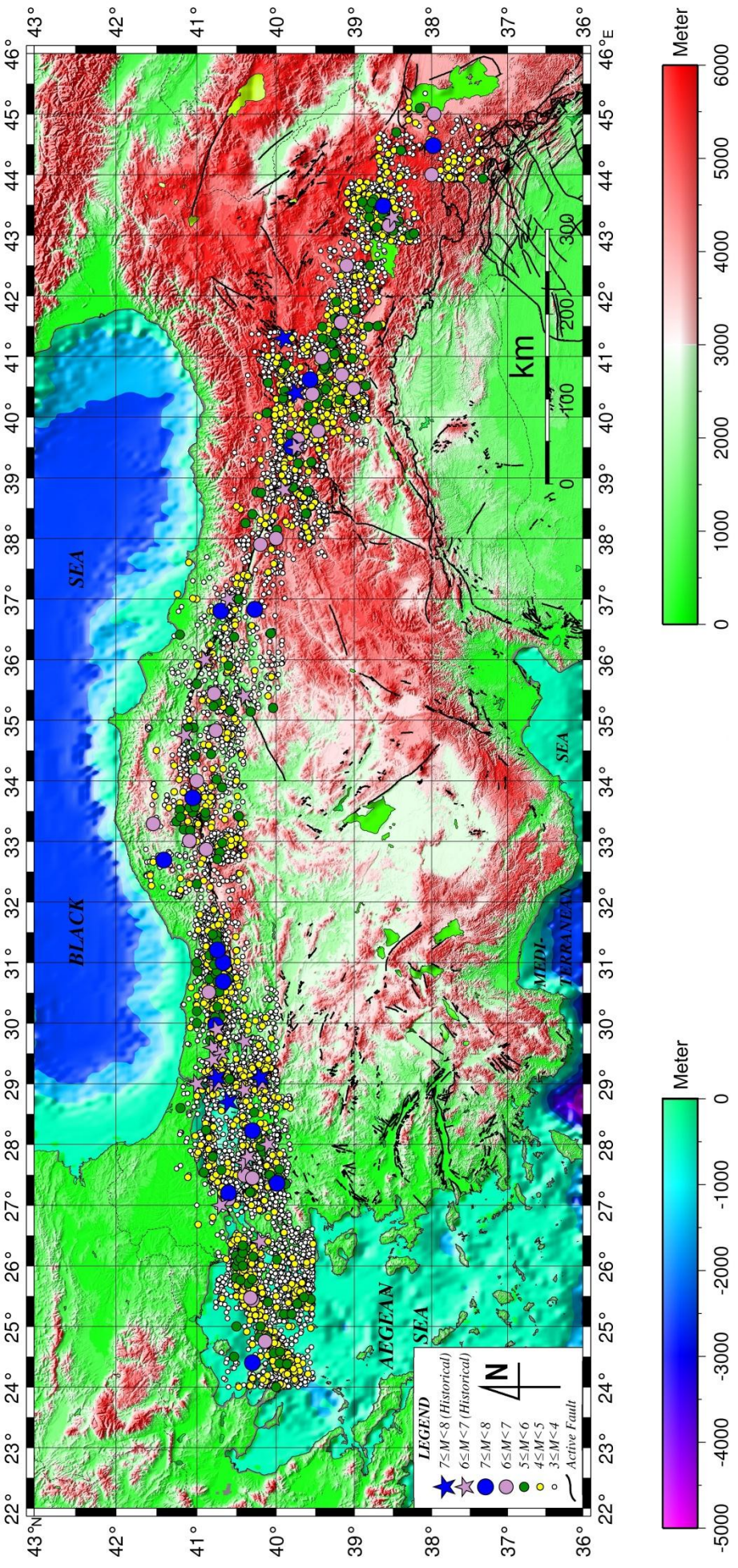

Figure 1. The epicenter map of North Anatolian Fault Zone and the earthquake data used. The epicenter distribution contains 13958 earthquakes with magnitude of 3 and greater in the period 0029/11/24 - 2014/12/31. Data is from the electronic earthquake catalogue of Boğaziçi University Kandilli Observatory and Earthquake Research Institute. Active faults on the map were to be put in order from Şaroğlu et al. (1992), and McClusky et al. (2000, 2003). The map was generated using GMT [61].

made according to both the entire instrumental period and the period when the earthquake observations in the instrumental period reached a specific standard, and the results for both periods have been compared.

II. METHOD and DATA

Seismic moment, one of the parameters defining the magnitude of an earthquake, is the moment of the equivalent force system that is active at the focus at the moment of an earthquake. The amplitude of the seismic waves caused by the equivalent force system is also proportional to seismic moment. Therefore, a linear relation as

$$\log M_0 = c + d\,M - e_M \tag{1}$$

can be sought between seismic moment and the magnitude of an earthquake. c and d are coefficients. e_M is the error parameter for log M_0. c and d constants may be found by regression analysis performed by means of the Least Squares Method. For this process, in this study, the curve fitting processes for some observed data were performed with two regression methods, namely standard least-squares regression (SR) and orthogonal regression (OR) [15]. The theoretical foundations for both methods are based on the minimization of the distances between observed values and the theoretical curve representing them. The first one is based on the minimization of the sum of squares of the distances between observed and calculated data, whereas the other one is based on the minimization of the sum of squares of the orthogonal distances between observed values and the theoretical curve. Statistically, a standard error is the ratio of the standard deviation of data to the square root of the number of data. So far, many researchers have provided such empirical equations for various regions. The operation is a first-order regression analysis and based on a calculation performed by means of the Least Squares Method. The error parameter is defined as the standard error, and if e_M is added to the two sides of an Equation (1) with zero error, Equation (1) can be rewritten as

$$\begin{aligned} \log M_0 + e_M &= (c + \delta c) + (d + \delta d)\,M, \\ e_M &= \delta c + \delta d\,M \end{aligned} \tag{2}$$

where δc and δd are the standard errors of c and d, respectively. If a variable transformation like

$$\begin{aligned} y &= x_1 + x_2 M \;; \\ y &= \log M_0 + e_M \;,\; x_1 = c + \delta c \;,\; x_2 = d + \delta d \end{aligned} \tag{3}$$

is performed in Equation (2), Equation (3) can be once more rewritten in matrix notation as

$$\mathbf{y} = \mathbf{M}\,\mathbf{x} \tag{4}$$

where **y** and **x** each are column vectors with dimensions (n × 1) and (2 × 1), respectively. n is the number of data, and **M** is a rectangular matrix with dimension (n × 2). Given this, the solution of Equation (4) can be expressed as

$$x = (M^T M)^{-1} M^T y \tag{5}$$

where superscript T shows the transpose of matrix **M**. If n is equal to 2, the solution of Equation (4) is performed as a full determined system. However, the number of data in this case is not reliable. Equation (5) can be calculated with miscellaneous methods. The LU decomposition method is used for Equation (5) in this study. Standard errors (δc, δd) are determined using both solution results calculated with Equations (5) and (3). On the other hand, the operations between Equations (2) and (5) mean the removal of the standard error from a regression function estimated according to the distribution of data.

Seismic moment is defined as

$$M_0 = \mu\,\bar{u}\,A \;,\; A = L \times W \tag{6}$$

[1]. μ is the rigidity coefficient, $\bar{u}$ the mean relative displacement taking place along the fault plane, and A the area of the fault plane. L denotes the length of the fault plane, while W denotes the width of the fault plane and corresponds to focal depth (H) in computations. Under Equation (6), it is possible to seek a relation similar to Equation (1) between seismic moment and the area of the fault plane. The equation related to this will be

$$\log M_0 = v + w\,A - e_A \tag{7}$$

where v and w are coefficients. e_A is the error parameter for Equation (7). To both estimate these coefficients and calculate their standard errors, the operations between Equations (2) and (5) are performed for Equation (7).

The total displacement occurring along a strike-slip fault at a specific time (D) is given with the equation

$$\Sigma u = \frac{1}{\mu}\Sigma M_0 \tag{8}$$

[11]. Considering this, the mean displacement velocity can be simply computed with the operation

$$\Omega = \frac{\Sigma u}{D} \tag{9}$$

The difference between the stresses before and after the dislocation caused by an earthquake is called stress drop. Considering the average dislocation definition by Brune and Allen (1967), the stress drop for a strike-slip fault can be calculated with the equation

$$\Delta\tau = \frac{2}{\pi}\frac{M_0}{AH} \tag{10}$$

In total, 29 earthquakes with $m_{b,s} \geq 4.8$, which occurred in the tectonic belt concerned in the 1909-2000 period and the macroseismic and instrumental observations of which were made, are used for the empirical relations, displacement, displacement velocity, and stress drop estimated using Equations (1) and (6)-(10). Table 1 shows these earthquakes in chronological order. The *

Table 1. The list of the earthquakes used in this study with macroseismic parameters, and their macroseismic and instrumental parameters. H, L, U_m, A and $\Delta\tau$ are the average focal depth of the fault, length of the elementary fault, amount of maximum relative dislocation of the elementary fault, fault area and stress-drop, respectively. * shows the not observed values.

ID	DATE (y / m / d)	LAT. (° N)	LON. (° E)	H (km)	m_b	M_s	L (km)	U_m (cm)	M_0 ($\times 10^{26}$ dyne-cm)	A (km^2)	$\Delta\tau$ (bar)	References[1]
01	1909.02.09	40.00	38.00	15.0*	6.3	-	15.0	-	1.2000*	225	-	Eyidoğan vd.,1991
02	1912.08.09	40.50	27.00	15.0*	-	7.4	60.0	-	6.1000*	900	-	Eyidoğan vd.,1991
03	1939.12.26	39.80	39.51	20.0	-	8.0	300.0	370.0	41.0000	6000	29	Kalafat vd.,2009; Ezen, 1981
04	1942.12.20	40.87	36.47	10.0	-	7.0	50.0	175.0	3.2000	500	27	Kalafat vd.,2009; Ezen, 1981
05	1943.11.26	41.05	33.72	10.0	-	7.3	280.0	150.0	16.0000	2800	24	Kalafat vd.,2009; Ezen, 1981
06	1944.02.01	41.41	33.69	10.0	-	7.3	180.0	350.0	23.0000	1800	54	Kalafat vd.,2009; Ezen, 1981
07	1946.05.31	39.30	41.20	15.0*	6.0	5.7	30.0	-	0.0540*	450	-	Eyidoğan vd.,1991
08	1949.08.17	39.35	40.60	15.0*	6.8	6.9	38.0	-	1.5000*	570	-	Eyidoğan vd.,1991
09	1951.08.13	40.88	32.87	10.0	7.0	6.9	60.0	-	0.9886	600	7	Kalafat vd.,2009; Eyidoğan vd., 1991
10	1953.03.18	39.99	27.36	10.0	-	7.5	50.0	430.0	8.0000	500	68	Kalafat vd.,2009; Ezen, 1981
11	1957.05.26	40.67	31.00	10.0	-	7.0	40.0	160.0	2.4000	400	25	Kalafat vd.,2009; Ezen, 1981
12	1963.09.18	40.77	29.12	40.0	6.2	6.3	-	-	0.2483	-	-	Kalafat vd.,2009; Eyidoğan vd., 1991
13	1964.10.06	40.30	28.23	34.0	5.9	6.9	40.0	-	0.2483	600	2	Kalafat vd.,2009; Eyidoğan vd., 1991
14	1966.08.19	39.17	41.56	26.0	5.8	6.8	60.0	30.0	0.6800	900	3	Kalafat vd.,2009; Ezen, 1981
15	1967.07.22	40.67	30.69	33.0	6.0	6.9	80.0	190.0	5.6000	1200	20	Kalafat vd.,2009; Ezen, 1981
16	1967.07.26	39.54	40.38	30.0	5.6	6.0	4.0	-	0.0881	60	6	Kalafat vd.,2009; Eyidoğan vd., 1991
17	1968.09.03	41.81	32.39	5.0	5.7	6.5	-	-	0.1245	-	-	Kalafat vd.,2009; Eyidoğan vd., 1991
18	1971.05.22	38.85	40.52	3.0	5.9	6.7	38.0	25.0	0.1758	114	7	Kalafat vd.,2009; Eyidoğan vd.,1991; KOERI[2]
19	1983.07.05	40.38	27.04	15.0	5.7	6.1	-	-	0.1600	-	-	Kalafat vd.,2009; Eyidoğan vd., 1991
20	1983.11.18	39.55	39.03	10.0	4.8	5.0	-	-	0.0160	-	-	Kalafat vd.,2009; KOERI
21	1992.03.13	39.94	39.57	15.0	6.2	6.8	-	-	1.2000	-	-	Kalafat vd., 2009
22	1992.03.15	39.52	39.84	15.0	5.5	5.8	-	-	0.0760	-	-	Kalafat vd., 2009
23	1996.08.14	40.52	35.02	15.0	5.3	5.6	-	-	0.0460	-	-	Kalafat vd., 2009
24	1998.04.13	39.18	41.10	15.0	4.8	4.8	-	-	0.0092	-	-	Kalafat vd., 2009
25	1999.08.17	40.76	29.97	17.0	6.3	7.8	150.0	500.0	29.0000	2550	35	Kalafat vd.,2009; KOERI; USGS[3]
26	1999.09.13	40.31	30.29	15.0	5.8	5.8	-	-	0.0600	-	-	Kalafat vd.,2009; KOERI
27	1999.11.11	40.95	30.10	15.0	5.5	5.5	-	-	0.0360	-	-	Kalafat vd.,2009; KOERI
28	1999.11.12	40.74	31.21	18.0	6.3	7.5	40.0	400.0	6.7000	440	38	Kalafat vd.,2009; KOERI; USGS
29	2000.06.06	40.75	32.70	15.0	5.5	6.1	-	-	0.1100	-	-	Kalafat vd.,2009; KOERI

[1]: for columns between 2-10
[2]: **K**andilli **O**bsevatory and **E**arthquake **R**esearch **I**nstitute
[3]: **U**nited **S**tates **G**eological **S**urvey

sign in Table 1 denotes the non-observed values. That is, they are the values generated depending on the empirical equations estimated within the scope of this study in order to use them in appropriate calculations. The first 10 columns in Table 1 contain the classical earthquake and source parameters and the macroseismic parameters belonging to the earthquakes used. Columns 11 and 12 in Table 1 are the parameters estimated within the scope of this study. On the other hand, the last column of Table 1 indicates the source of the data belonging to the first 10 columns. The first 18 earthquakes until 05/22/1971 in Table 1 are the earthquakes that are also used in the studies by Canıtez and Ezen (1973) and Ezen (1981), and 8 of them are comprised of data based on observed parameters, while the rest are comprised of data based on derived parameters.

The Gutenberg-Richter magnitude-frequency equation is the most fundamental equation in seismicity analysis and it is expressed as

$$\log N(M) = a - bM \tag{11}$$

[26], [25]. N is the number of earthquakes with minimum magnitude M in observation period D, whereas a and b are regression coefficients. a and b constants may be found by regression analysis. Considering Equation (11), the optimum distribution for the regional earthquake hazard analysis is Gumbel (Extreme Value Type I) distribution defined as

$$G(M) = \exp\left[-\alpha \exp(-\beta M)\right] \ , \ M > 0 \tag{12}$$

[24]. α and β are Gumbel regression coefficients. Gumbel (Extreme Value Type I) was preferred owing to the unique nature of the earthquake data and the use of maximum magnitudes in the hazard analysis and as these calculations were performed in a regional area. From Equation (12), the probability of occurrence of an earthquake with magnitude M in D years can be expressed as

$$R(D) = 1 - G(M, D) \tag{13}$$

Equation (13) is the probability of exceedance or seismic risk of an earthquake with magnitude M in a period of D years. In this case, the return period of probable magnitudes in a region is the opposite of the annual risk. In this study, the earthquake catalogue of the data bank of Kandilli Observatory and Earthquake Research Institute of Boğaziçi University was used for seismicity and earthquake hazard analyses.

III. EMPIRICAL EQUATIONS

In this section, the empirical relations between some earthquake source parameters are estimated according to the latest seismological and macroseismic data about the NAFZ in order to monitor the development of the seismological activity in a specific period.

A. Seismic Moment-Magnitude Relation in the North Anatolian Fault Zone

When estimating the relation between seismic moment and magnitude under Equation (1), this operation is considered according to both m_b and M_s. When the necessary regression analysis is made according to Equation (1), the relations

$\log M_0 = 15.427\ [\pm 0.11] + 1.736\ [\pm 0.07 \times 10^{-4}]\ m_b$; *(4.8 ≤ m_b ≤6.3)*, σ= 0.47, e= 0.056, r= 0.85
(for SR) (14a)

$\log M_0 = 13.607\ [\pm 0.12] + 2.055\ [\pm 0.07 \times 10^{-4}]\ m_b$; *(4.8 ≤ m_b ≤6.3)*, σ= 0.49, e= 0.051, r= 0.85
(for OR) (14b)

$\log M_0 = 17.634\ [\pm 0.13] + 1.340\ [\pm 0.88 \times 10^{-4}]\ m_b$; *(6.3 < m_b ≤7.0)*, σ= 0.54, e= 0.075, r= 0.78
(for SR) (14c)

$\log M_0 = 15.457\ [\pm 0.13] + 1.716\ [\pm 0.35 \times 10^{-4}]\ m_b$; *(6.3 < m_b ≤7.0)*, σ= 0.58, e= 0.067, r= 0.78
(for OR) (14d)

$\log M_0 = 17.863\ [\pm 0.07] + 1.205\ [\pm 0.25 \times 10^{-4}]\ M_s$; *(4.8 ≤ M_s ≤8.0)*, σ= 0.35, e= 0.044, r= 0.94
(for SR) (14e)

and

$\log M_0 = 17.390\ [\pm 0.07] + 1.277\ [\pm 0.10 \times 10^{-4}]\ M_s$; *(4.8 ≤ M_s ≤8.0)*, σ= 0.35, e= 0.043, r= 0.94
(for OR) (14f)

are calculated between seismic moment and the body and surface wave magnitudes taking place along the NAFZ. M_0 is in dyne-cm. Standard errors are in the square brackets, and σ and r are the standard deviation and the correlation coefficient, respectively. e is the standard error calculated the according to the orthogonal distances for the regression function. Figures 2 and 3 show the changes in these correlations, respectively. As seen from both figures and from the correlation coefficients computed, there is a good fit between the estimated mathematical function and the observed values. Equations (14a,c,e) and (14b,d,f) are equations which are obtained with standard least-squares and orthogonal regression methods, respectively. As it is also seen from them, there is no significant difference between the results of orthogonal regression and standard regression, and their e values are the nearly same values. Consequently, this no significant difference may not influence the interpretation for these equations.

The same relation, mentioned in both Canıtez and Ezen (1973) and Ezen (1981), is provided with equations

$\log M_0 = 17.00 + 1.33\ m_b$; *(6.0 ≤ m_b ≤8.0)*
(Canıtez and Ezen, 1973; Ezen, 1981) (15a)

and

$\log M_0 = 17.96 + 1.23\ M_s$; *(6.0 < M_s ≤8.0)*
(Ezen, 1981) (15b)

When Equations (14a,b,c,d) and (15a) are considered, it is seen that both equations define the same activity in the NAFZ. Nevertheless, the striking numerical differences in coefficients a and b result from the fact that the

magnitude values then are disputable today. The magnitude values used today for the earthquakes in use

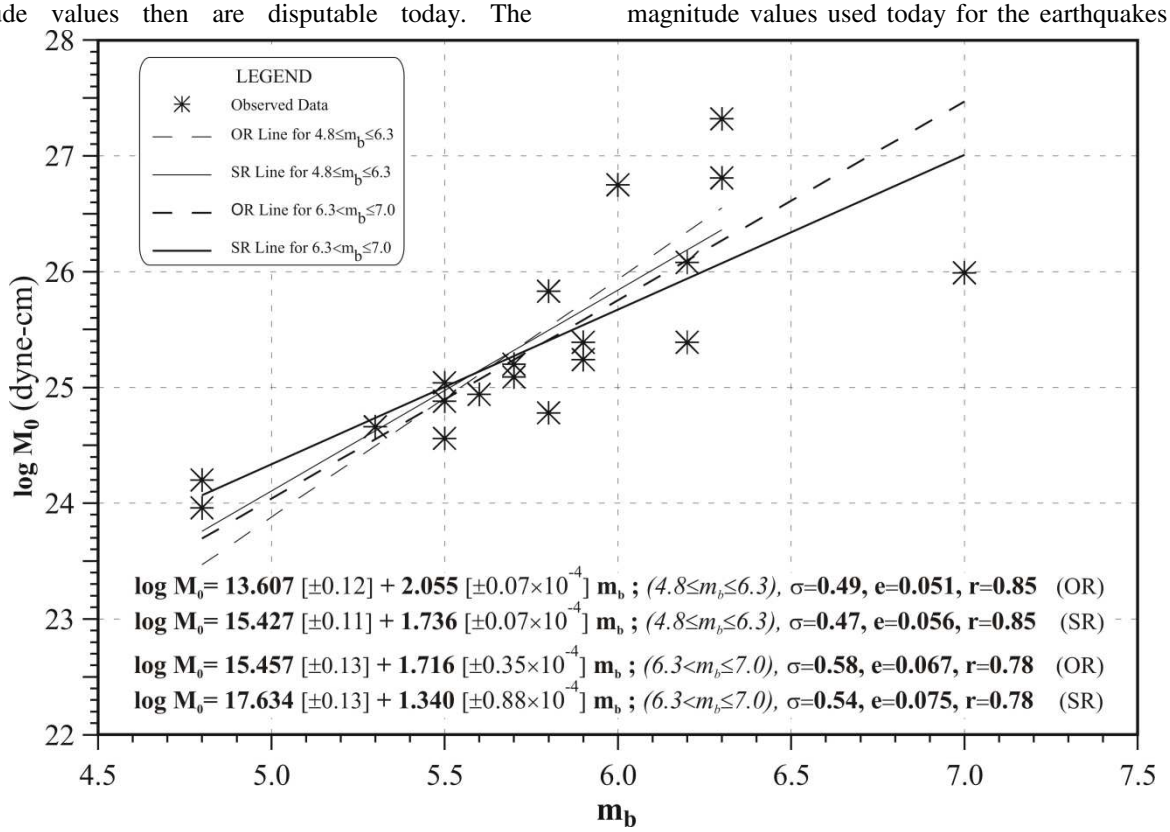

Figure 2. The seismic moment (M_0) - body wave magnitude (m_b) relation for the North Anatolian Fault Zone. It is for earthquakes with magnitude $4.8 \leq m_b \leq 7.0$. SR and OR stand for the **S**tandard Least-Squares **R**egression and **O**rthogonal **R**egression, respectively. Standard errors are in the square brackets, σ and r are the standard deviation and correlation coefficient, respectively. e is the standard error calculated the according to the orthogonal distances for the regression function.

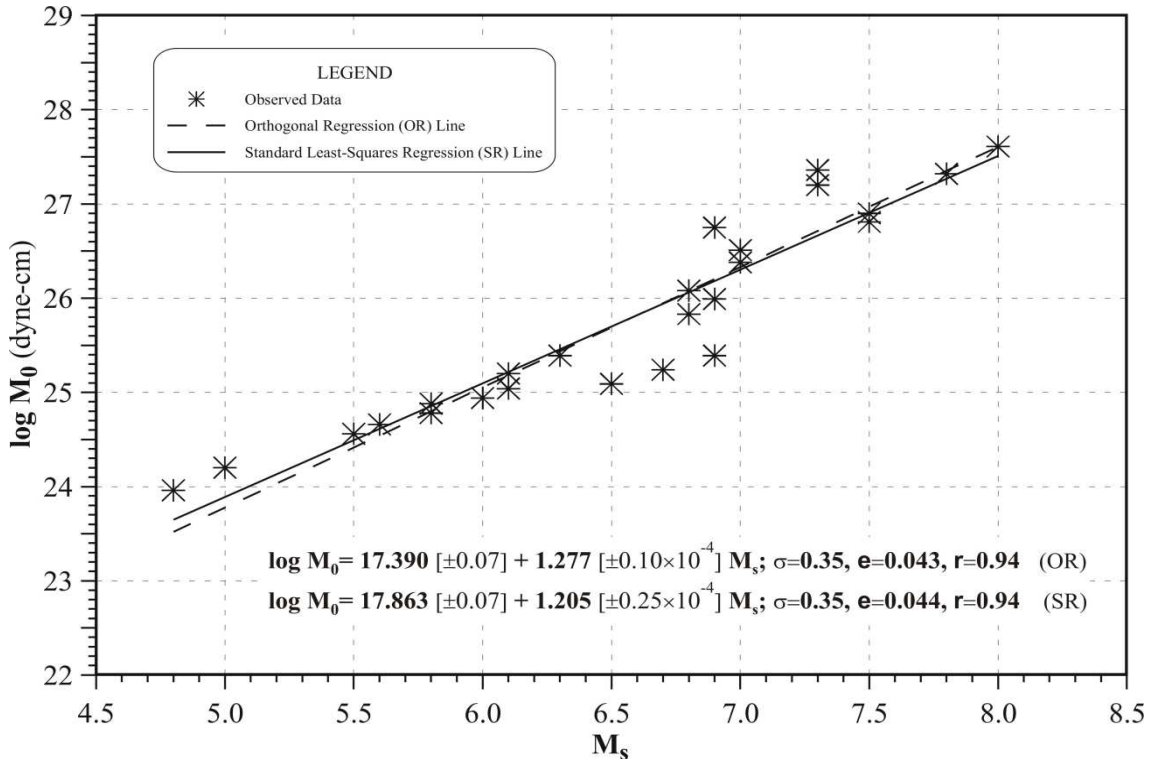

Figure 3. The seismic moment (M_0) - surface wave magnitude (M_s) relation for the North Anatolian Fault Zone. It is for earthquakes with magnitude $4.8 \leq M_s \leq 8.0$. Standard errors are in the square brackets, σ and r are the standard deviation and correlation coefficient, respectively. e is the standard error calculated the according to the orthogonal distances for the regression function.

involve fewer errors. When the relation according to the surface wave in Equations (14) and (15) is considered, it is seen that there is almost no difference between Equations (14e,f) and (15b). The difference mentioned here is a result of the use of more data, which we perceive as positive and rather as improvement. That is, the advantage of the number of data which has increased until this study since the previous studies is stated. If no change is observed, it also expresses that there has not been any noteworthy change yet notwithstanding the added data. However, when the relationship according to the surface wave is considered in Equations (14) and (15), it appears that there is hardly any difference between Equations (14e) and (15b). Nevertheless, Equation (14e) and the magnitude interval at which this equation is valid have expanded. This also applies to the other Equations (14a,b,c,d,e,f).

Then, the character of the NAFZ in the relation of seismic moment with magnitude remains unchanged even in the case of a change in the magnitude range in use. However, the interval of magnitude m_b is divided and further elaborated by this study, and the empirical equations concerned (14a,b,c,d) therefore acquire a more specific quality. So it means that the NAFZ has been maintaining its same character in terms of the seismic moment-magnitude relation approximately for the last ~30 years.

B. Seismic Moment-Fault Plane Relation in the North Anatolian Fault Zone

In the seismic moment-fault plane relation, the fault plane is calculated on the basis of fault length and focal depth. The mean focal depth assumed along the tectonic belt is used for the earthquakes with an unknown focal depth. When the relation concerned is computed under Equation (7) depending on the 15-km mean focal depth considered along the NAFZ in this study, it appears that the relation concerned did not display any single character and should be considered in two sections according to the different ranges of the magnitude concerned. The equations regarding this approach are computed as

$\log M_0 = 25.330\ [\pm 0.15] + 1.3 \times 10^{-3}\ [\pm 0.00]\ A$;
($4.8 \le m_b < 7.0$, $4.8 \le M_s < 7.6$), $\sigma = 0.58$, e= 0.155, r= 0.56
(for SR) (16a)

$\log M_0 = 24.761\ [\pm 0.18] + 2.30 \times 10^{-3}\ [\pm 0.00]\ A$;
($4.8 \le m_b < 7.0$, $4.8 \le M_s < 7.6$), $\sigma = 0.65$, e= 0.175, r= 0.56
(for OR) (16b)

$\log M_0 = 26.776\ [\pm 0.07] + 0.2 \times 10^{-3}\ [\pm 0.00]\ A$;
($m_b \ge 7.0$, $M_s \ge 7.6$) , $\sigma = 0.20$, e= 0.071, r= 0.86
(for SR) (16c)

and

$\log M_0 = 26.721\ [\pm 0.06] + 1.8 \times 10^{-4}\ [\pm 0.00]\ A$;
($m_b \ge 7.0$, $M_s \ge 7.6$) , $\sigma = 0.16$, e= 0.057, r= 0.86
(for OR) (16d)

where A is in km^2. Figure 4 shows the change in the seismic moment-fault plane relation, the mathematical expression of which is provided with Equations (16a,b,c,d). The correlation coefficients of Equations (16a,b) are not good. However, the available data are of that kind. As it is also seen from Equations (16a,b,c,d) there is no significant difference between the results of orthogonal regression and standard least-square regression. Equations (16a,b,c,d) do not undergo any significant change either when the mean focal depth is increased to 20 km.

Regarding the change in slope in Figure 4, first of all it can be stated that: Since the density gradually increases generally from the surface deeper into the Earth and hence the seismic wave rates also increase, it means that the Earth consists of the geological formations which gradually become stiffer from the surface deeper into the Earth. In other words, a looser material is available in the places close to the Earth's surface, whereas a stiffer material is available towards the deeper places. This is at least so in the lithosphere except for some singularities and the crustal rheology generally works so. According to such rheology, the rupture force will further deform the material perpendicularly upon progressing from shallow levels to deep levels or as the hypocenter deepens. That is, the width (W) of the rupture plane will start to grow more easily than its length (L). Hence, the longitudinal rupture takes place more easily in a shallow-focus earthquake that occurs in such a material, the characteristic feature of which has been emphasized above, than in a deep-focus earthquake because the longitudinal change in the material is concerned with the same level of stiffness on average. However, the transverse change in the material – i.e. towards the deeper place – is from a little stiff material to highly stiff material, and develops slowly as the resistance gradually increases. This issue is addressed in this line in Scholz (2002). That is, the seismic moment will change more slowly after the rupture plane area has reached a specific size. This difference in the rate of change is seen in the change in the slope of the regression line in Figure 4. This physical event is ultimately concerned with the size of the resultant fault plane because although it is stated in Scholz (2002) that the slip vector is proportional to the length (L) of the fault plane up to a specific fault length and, after this specific length, to the width (W) of the fault plane, L is also proportional to A and W is also proportional to A as A=L×W (L=A/W, W=A/L). That is, the slip vector is always indirectly proportional to the fault plane area. Hence, according to this specific length, the seismic moment will also be proportional to the values of the fault plane which are in specific sizes (Scholz, 2002). All the above-mentioned things mean the behavior of the material which conforms to physical rules. Accordingly, the change in moment slows down as the rupture plane grows (/increases) due to the attenuation of the rupture energy in time.

When compared with equations

$\log M_0 = 24.60 + 2.250 \times 10^{-3}\ A$; *($m_b < 7.0$)*
(Canıtez and Ezen, 1973) (17a)

and

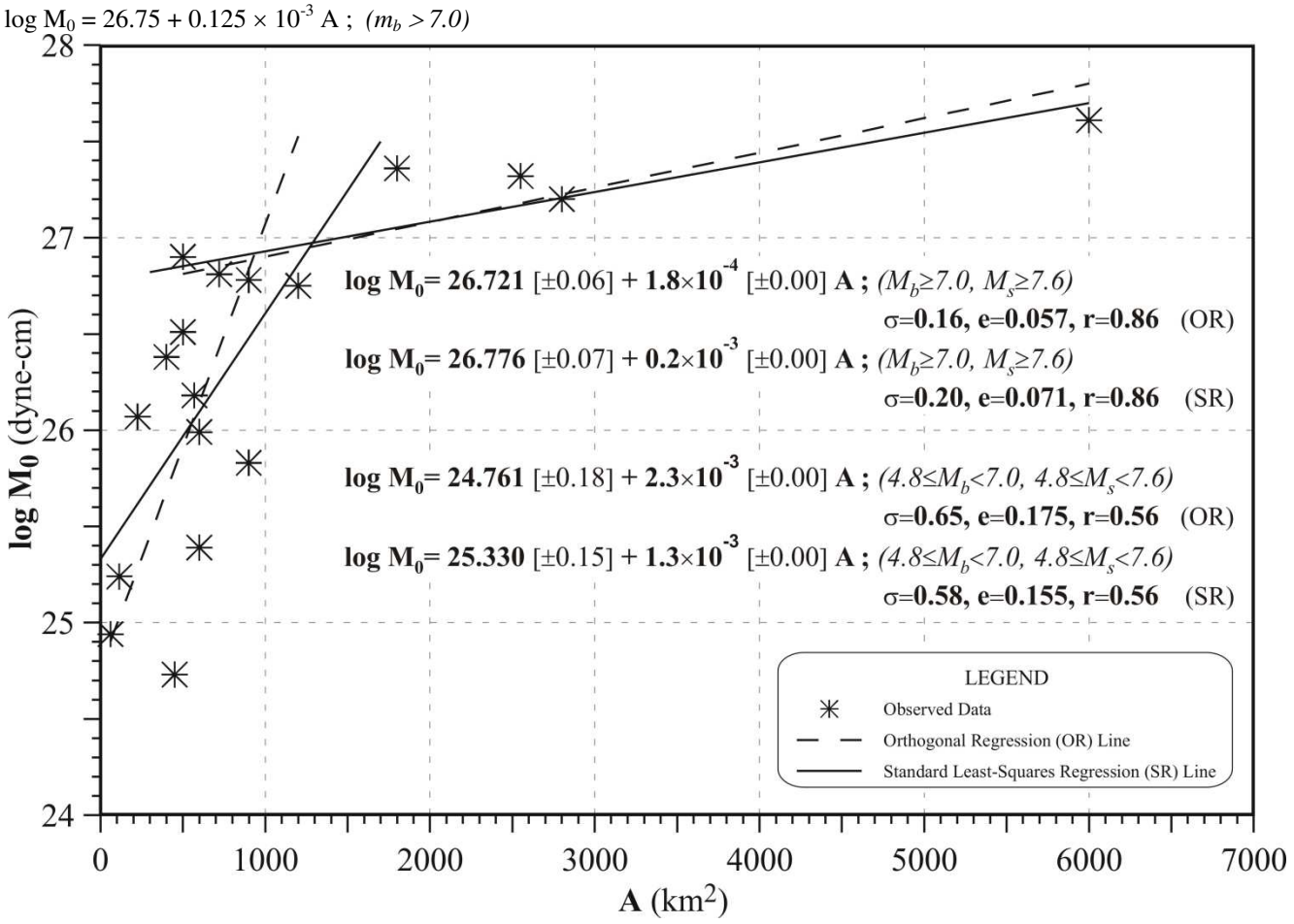

Figure 4. The seismic moment (M_0) - fault plane area (A) relation for the North Anatolian Fault Zone. Standard errors are in the square brackets, σ and r are the standard deviation and correlation coefficient, respectively. e is the standard error calculated the according to the orthogonal distances for the regression function.

(Canıtez and Ezen, 1973) (17b)

provided by Canıtez and Ezen (1973), a change that further slopes down in time is observed for ($m_b \leq 6.8$), while a change that further steepens is observed for *($m_b > 6.8$)*. Accordingly, it can be interpreted that the seismic moment remains at a value which fits the magnitude for earthquakes of moderate magnitude and that a greater seismic moment occurs for major earthquakes again due to the same fit. In other words, it might be stated that along the NAFZ, those earthquakes in which small fault planes occur have small moments, whereas those earthquakes in which large fault planes occur have large moments. From these results, it is seen that one approaches a more accurate character as the number of data in use increases. Moreover, by using Equation (16a), the threshold magnitude value required to observe a surface fault to result from the earthquakes that will occur along the NAFZ is calculated to be either 5.7 (m_b) or 6.2 (M_s) when A = 0. Canıtez and Ezen (1973) give the value of 5.7 (m_b) for this parameter.

IV. KINEMATIC CHARACTERISTICS

The North Anatolian Fault Zone is a transform fault zone where shallow seismic activity prevails and where the seismic focal depths mostly reach a maximum of 20 km, whereas the depths of daily microseismicity are below 10 km. With its minimum length of 1400 km, its deformation area of up to 10 km in some places, and its main dominant rightward strike-slip mechanism, the NAFZ plays an essential role in the regional tectonism. Such kinematic parameters as stress drop, total displacement, and displacement velocity are guiding parameters in a fault mechanism. The displacement velocity is investigated according to the possible values of the parameters of fault zone length and focal depth – which are determining elements in Equations (1) and (6)-(10) – that fit the characteristics of the fault zone concerned.

A. Stress Drop in the North Anatolian Fault Zone

When computing the stress drops at the 29 epicenter points along the NAFZ that are considered within the scope of this study, the seismic moments of the elementary faults and the elementary fault geometries (L,W) are used under Equation (10). During the calculations of stress drop provided in Column 12 of Table 1, the length of the NAFZ and its mean focal depth were considered 1400 km and 15 km, respectively. The values concerned are based on the principle of best representing the data in Table 1 used in these

calculations. From the results obtained, it is seen that the stress drop along the NAFZ ranges from 2 to 68 bars (Table 1). In other words, the stress drop in the NAFZ varies at the level of 10s according to the earthquakes with $4.8 \leq m_b \leq 7.0$ or $4.8 \leq M_s \leq 8.0$ in the 1909-2000 period. This feature is in agreement with the mean focal depth of 15 km, assumed along the NAFZ. That is, the NAFZ generates shallow-focus earthquakes. This result is based on the view that the stress drops between 0 and 100 bars are related to shallow-focus earthquakes, which is expressed by Aki (1972). Figure 5 shows the epicenters of the 29 earthquakes used in this study and the change in stress drops calculated along the NAFZ. Along the zone concerned, the place between Çanakkale and Balıkesir, the surroundings of İzmit, Sakarya and Bolu, the place between Kastamonu and Bartın, the place among Samsun, Amasya and Tokat and the place among Erzincan, Karlıova (Bingöl) and Tunceli indicate the places for which the highest stress drops are calculated. On the other hand, the other areas on the zone do not yield any significant stress drop. This can be accounted for by the fact that the process of storage of strain energy has not been completed yet or by the creep event.

The change in stress drops seen in Figure 5 differs from the change observed in the study by Canıtez and Ezen (1973) in that the highest value of stress drop increases from 35 bars to 68 bars in Figure 5 and in that the surroundings of İzmit and Sakarya are included in the south-west of the Kapıdağ Peninsula and Erzincan (Figure 5) with a high value in Canıtez and Ezen (1973). The place between Çanakkale and Balıkesir with 68 bars is dominant in Figure 5.

B. Slip Rate in the North Anatolian Fault Zone

The total amount of slip and the mean slip rate in the NAFZ are computed on the basis of the activity period of the data in Table 1 with Equations (8) and (9), respectively. The calculations were made for the possible fault zone lengths and the possible mean earthquake focal depths for the NAFZ. In these calculations, it was considered that $\mu = 3.3 \times 10^{11}$ dyne/cm^2. Table 2 presents the related parameter values used in calculations, the total amounts of displacement obtained, and the mean displacement velocities. As also seen from Table 2, the total amount of slip ranges from 105.9 to 368.3 cm, whereas the slip rate ranges from 1.2 to 4.0 cm/year. From the distribution of epicenters of the data used (Table 1), it is seen that the most significant fault zone length for this data is 1400 km. Likewise, from the distribution of focal depths of the data used, it is understood that the most significant mean focal depth is 15 km and it is at least seen that it is below 20 km. Considering this, the fault zone length of 1150 km is short due to the earthquakes around the Biga Peninsula in Figure 5. In other words, this length of 1150 km does not duly represent the data.

Canıtez and Ezen (1973) give the mean slip rate as 2.4 cm/year (Table 2) according to a focal depth of 20 km and a fault zone length of 1600 km and they provide the values of 1.6 and 1.2 cm/year for the same length and for the focal depths of 30 and 40 km, respectively. The focal depths greater than 20 km here are thought-provoking and they were probably included out of curiosity. For the length they used, Canıtez and İlkışık (1973) state that it is the distance from Lake Van to the western end of the Fault. Thus, the value of 2.2 cm/year obtained according to the fault zone length of 1400 km and the mean focal depth of 15 km should be considered the most significant mean slip rate for the NAFZ (Table 2).

V. SEISMICITY

The NAFZ is one of the important transform systems in the world and easily manifests itself within the distribution of epicenters in and around Turkey in terms of its extension and deformation area. According to the catalogue used, it has generated some 13958 earthquakes with a minimum magnitude of 3 between 11/24/0029 and 12/31/2014. The 1529 of this are earthquakes with magnitudes 4.0 and greater. Also considering the error limits of the procedure of earthquake cataloging, it is appropriate to put the word “minimum” for the number of earthquakes that occurred. The number of earthquakes provided corresponds to a fault zone length of 2000 km. Of this number, 39 are historic earthquakes, 5 with intensity X and 34 with intensity IX. Figure 6 shows the distribution of epicenters of the NAFZ according to some 13958 earthquakes with a minimum magnitude of 3 between 11/24/0029 (29 A.D.) and 12/31/2014 and the fault plane solutions of 55 earthquakes ($4.2 \leq M_s \leq 7.8$), the **C**entroid **M**oment **T**ensor (CMT) inversion of which was made. The Map of Epicenters in the North Anatolian Fault Zone in Figure 6 was prepared with the GMT (The Generic Mapping Tools; Wessel and Smith, 2006). The active faults on the map were arranged from the studies by Şaroğlu et al. (1992) and by McClusky (2000, 2003). The CMT solutions belong to Harvard University (http://www.seismology.harvard.edu/). According to the earthquakes with minimum magnitude 4, there were 1529 earthquakes in the same period, with the historic ones being identical. When the fault zone length is considered 1600 km, the number of earthquakes with a minimum magnitude of 3 is 11612 and the number of earthquakes with a minimum magnitude of 4 is 1270. The number of historic earthquakes within both is 38, 5 with intensity X and 33 with intensity IX. When the fault zone length is considered 1400 km, the number of earthquakes with a minimum magnitude of 3 is 9696 and the number of earthquakes with a minimum magnitude of 4 is 1050. The number and content of historic earthquakes are the same as those in the case of 1600 km. The same period applies to both.

When the distribution of stations of the national observation network, on which the catalogue used is based, and its frequency development periods are taken into consideration, it is seen that the 115-year instrumental period between 1900 and 2014 and the 38-year recent period between 1977 and 2014 are considered individually for the earthquake generation analysis of the NAFZ. During the analyses concerned, the data used were eliminated from the aftershocks and a completeness

analysis was made. The process of eliminating from the aftershocks is a declustering process. Figure 7 illustrates

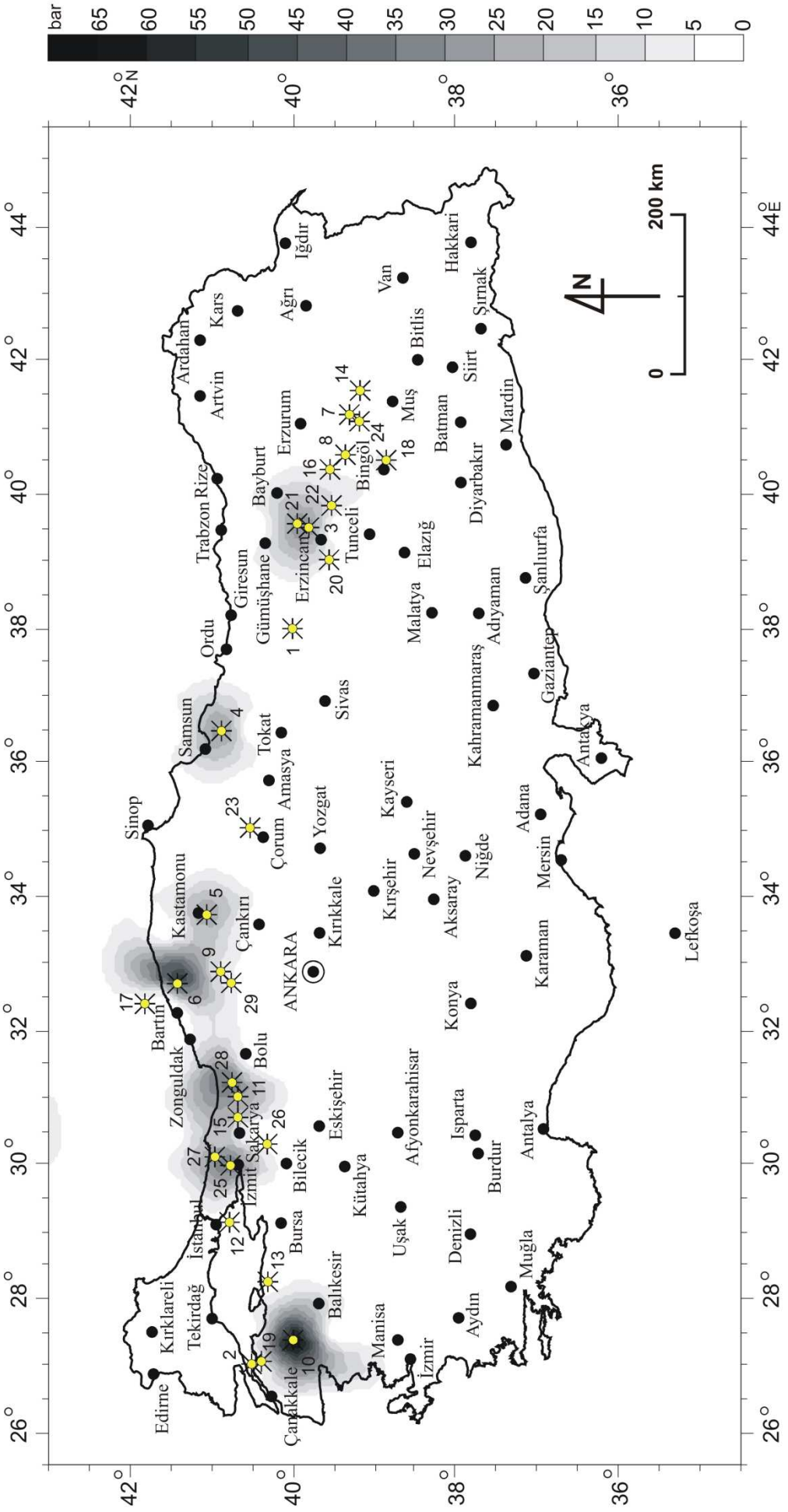

Figure 5. The variation of stress-drop along North Anatolian Fault Zone. Color scale is in bar. ✳ shows the epicenters of earthquakes studied.

Table 2. A comparison of the average slip rate. H, ∑L, ∑u and Ω are the average focal depths, length of the fault zone, amount of total dislocation on the fault zone and average slip rate, respectively.

ID	YEAR RANGE	*PERIOD (year)*	**ΣL** *(km)*	**H** *(km)*	**Σu** *(cm)*	**Ω** *(cm/year)*	**References**
01	1909-1999	91	1150	10	368.3	4.0	This study (2018)
02				15	245.5	2.7	
03				20	184.2	2.0	
04			1400	10	302.5	3.3	
05				15	201.7	2.2	
06				20	151.3	1.7	
07			1600	10	264.7	2.9	
08				15	176.5	1.9	
09				20	132.4	1.5	
10			2000	10	211.8	2.3	
11				15	141.2	1.6	
12				20	105.9	1.2	
13	1900-1971	72	1600	20	169	2.4	Canıtez and Ezen (1973)

the process for magnitude 3.0. In Figure 7, it is shown the frequency distribution according to years of magnitudes 3.0 and greater for the North Anatolian Fault Zone that the length of 2000 kms between 1900 and 2014. The cumulative curve and its fitting function is a very important knowledge for declustering. The cumulative frequency is the total absolute frequency of all values more than that boundary. It is the running total of frequency. As seen also from Figure 7, the years 1983, 1999, 2003 and 2011 has a clustering of seismicity. The declustering process is performed by the fitting function estimated during the analysis. The data were cleaned off the aftershocks on the basis of the modified Omori Law (Utsu et al., 1995). The completeness analysis was applied to the magnitudes in the sense of the peak value of the first derivative of the magnitude-frequency curve. Figure 8 is an exemplification showing the position of the magnitude of completeness (Figure 8a, Figure 8b). The figure shows the distribution of cumulative numbers of earthquake which corresponding to the magnitudes used. Also this example is for the North Anatolian Fault Zone that the length of 2000 kms between 1900 and 2014, and Figure 8 includes the earthquakes with magnitudes 3.0 and greater. The lower limit of the reliable magnitude represented with the completeness magnitude in Figure 8a seems as if it was possible in only one place on the data. Likewise, the ordinate axis on this figure is linear. If the ordinate axis is logarithmic, it will be seen that the available observed data require one more magnitude limitation. This requirement is seen in Figure 8b. Figure 8b shows the variations of the cumulative frequencies drawn according to the logarithmic ordinate axis which correspond to the magnitudes. As also seen from Figure 8b, the magnitudes greater than 6.5 are the magnitudes which do not conform to the earthquake occurrence regime in the middle part of the data ($3.5 \leq M \leq 6.5$), i.e. which occur more infrequently in comparison with this regime, and they upset the linear variation of the data or change the character of the data. On the other hand, the first part of the data, i.e. the earthquakes smaller than magnitude 3.5, comprises the earthquakes which occur more frequently as compared with the middle part that characterizes the data. In other words, the completeness magnitude is an important parameter which applies to both ends of the data. Considering this, the completeness magnitude was not used as a unique parameter in this study. Since the completeness magnitude was individually important for both ends of the data, a completeness magnitude was also used for the last part of the data in the appropriate data. They are available in Tables 3 and 4. Given this reality, these two values were called the *completeness magnitude*

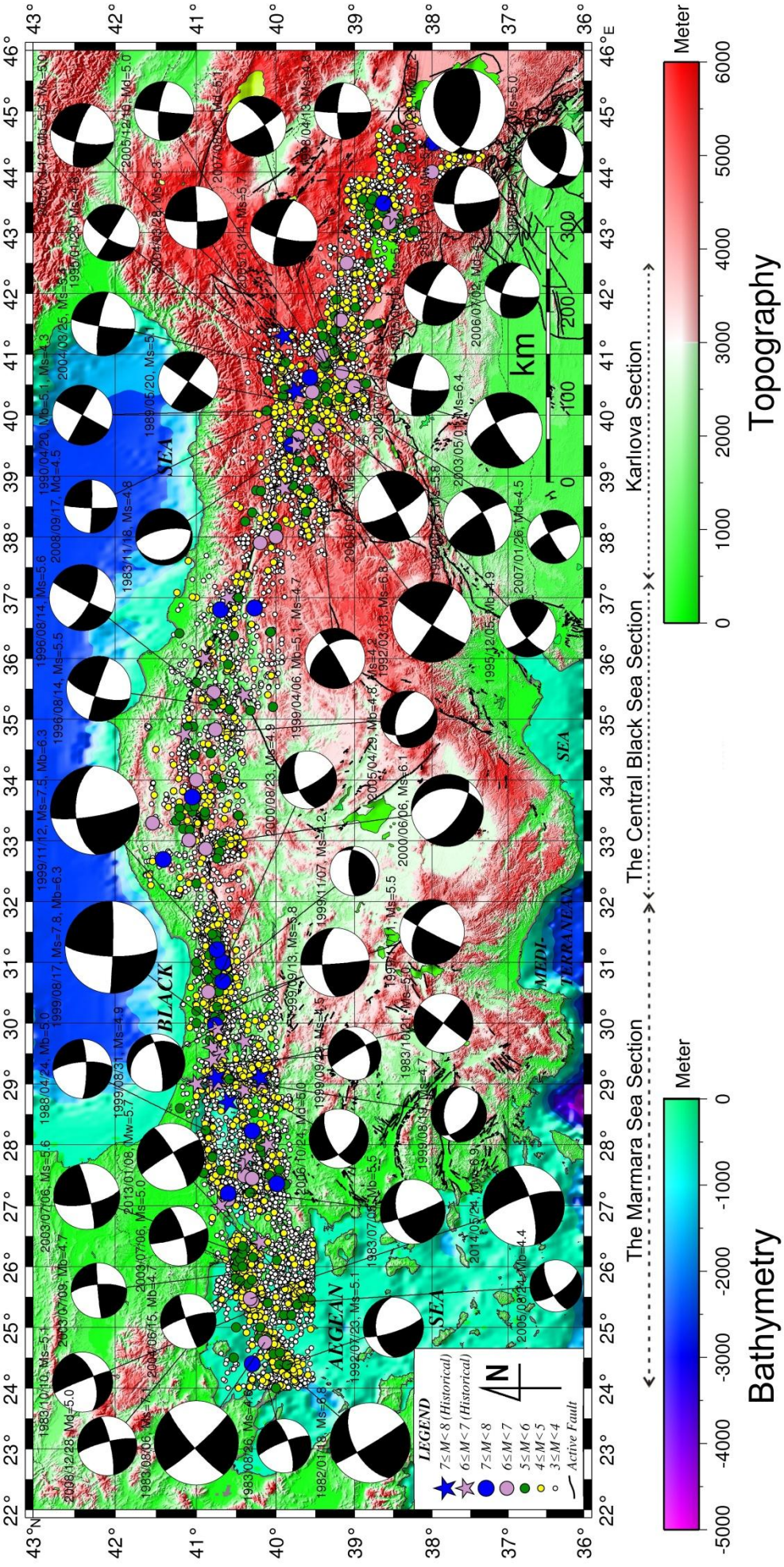

Figure 6. The fault plane solutions and epicenter distribution of North Anatolian Fault Zone. The epicenter map is based to 13958 earthquakes with magnitude of 3 and greater in the period 0029/11/24 - 2014/12/31. Data is from the electronic earthquake catalogue of Boğaziçi University Kandilli Observatory and Earthquake Research Institute. There are 55 earthquakes ($4.2 \leq M_s \leq 7.8$) with the fault plane solution. Fault plane solutions are Centroid Moment Tensor solutions made by Harvard University. Dark quadrants in the mechanism diagrams correspond to the compressional areas in the free surface. The representations are lower hemisphere, equal-area projections on the focal sphere. Active faults on the map were to be put in order from Şaroğlu et al. (1992), and McClusky et al. (2000, 2003). The map was generated using GMT [61].

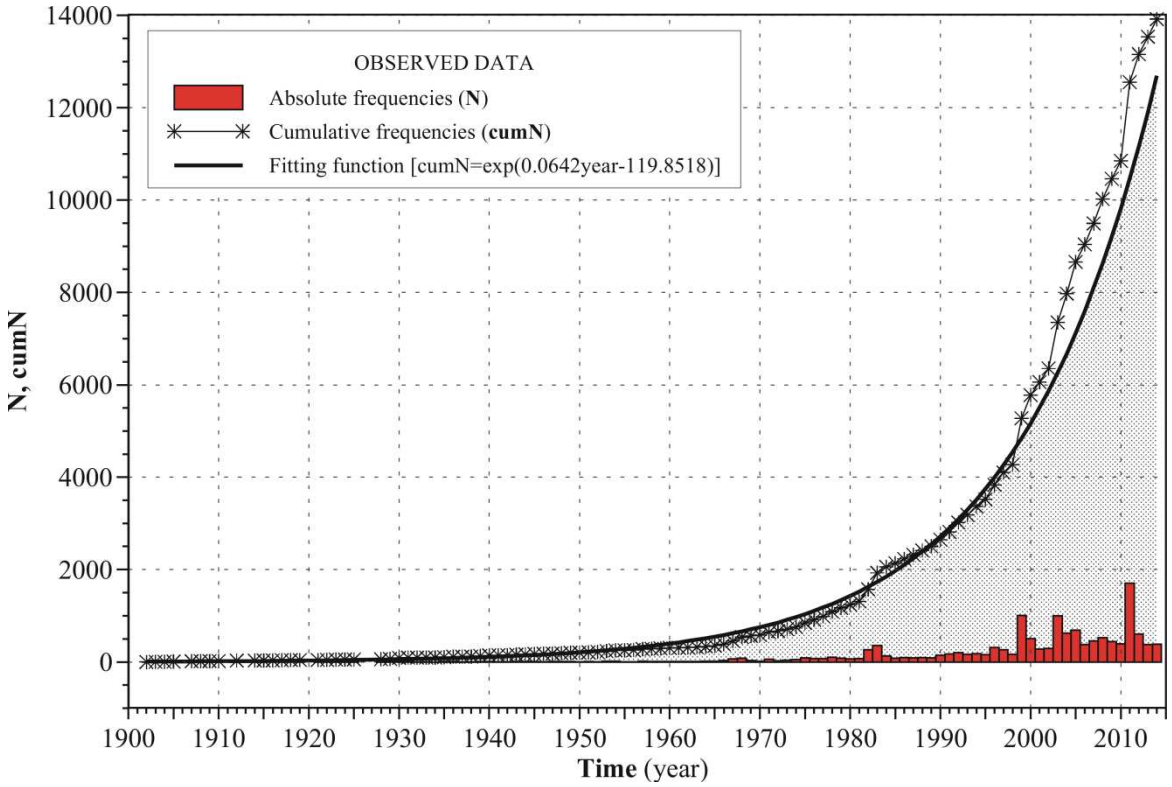

Figure 7. The cumulative frequency distribution and its fitting function, and the absolute frequencies according to time for the earthquakes with magnitudes 3.0 and greater occurred in the North Anatolian Fault Zone which has length of 2000 kms between 1900 and 2014. N and cumN are the absolute and cumulative numbers of earthquakes, respectively. Data is from the electronic earthquake catalogue of Boğaziçi University Kandilli Observatory and Earthquake Research Institute.

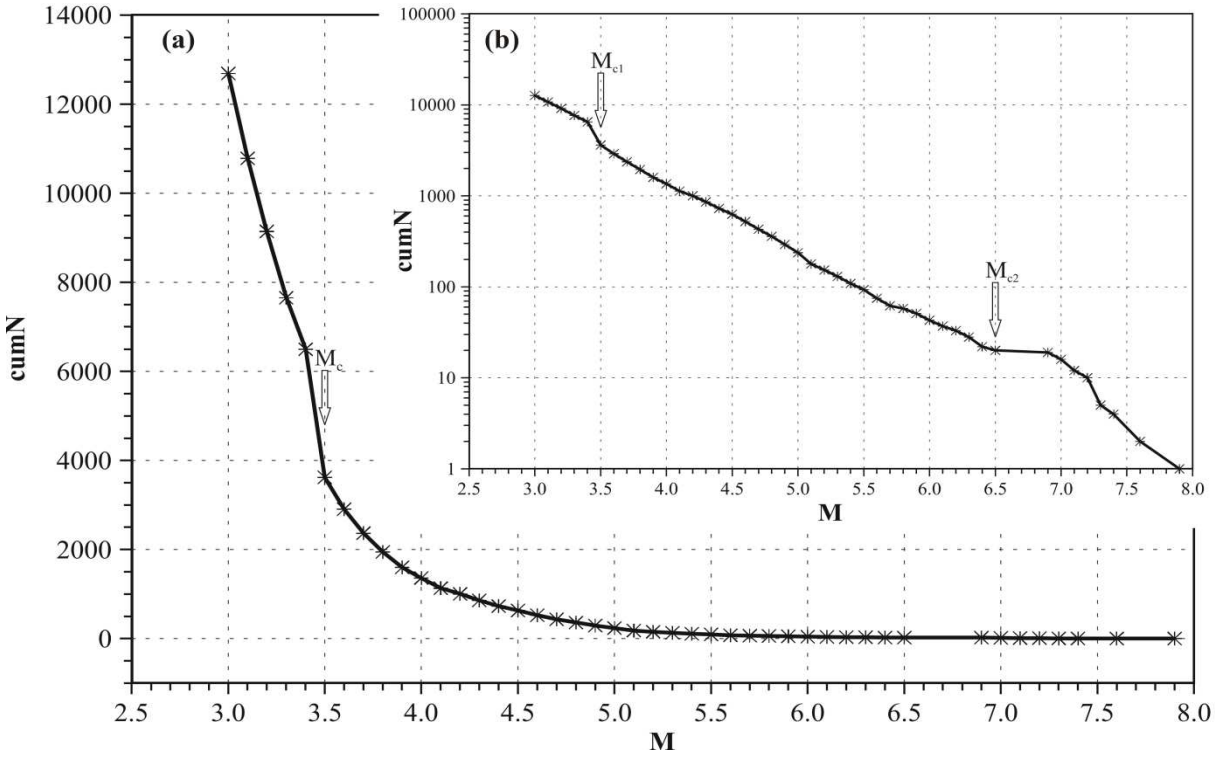

Figure 8. The cumulative frequency distribution which correspond to the magnitudes for the length of 2000 kms of North Anatolian Fault Zone in terms of the earthquakes with magnitudes 3.0 and greater between 1900 and 2014. cumN and M_c are the cumulative number of earthquakes and the magnitude of completeness, respectively. **(a)** The variations of the cumulative frequencies drawn according to the linear ordinate axis. **(b)** The variations of the cumulative frequencies drawn according to the logarithmic ordinate axis. (M_{c1}, M_{c2}) is a completeness magnitude pair. Data is from the electronic earthquake catalogue of Boğaziçi University Kandilli Observatory and Earthquake Research Institute.

pair in this study. (M_{c1}, M_{c2}) shown in Figure 8b is a completeness magnitude pair. Table 3 shows the earthquake generation analysis made according to these periods. From the sequences of epicenters in Figure 6, sub-sections were formed on the fault zone for the seismicity analysis of the fault zone concerned. As also seen from Figure 6, they are the Marmara Sea Section, the Central Black Sea Section, and Karlıova Section. These sub-sections in the NAFZ are defined in Table 3. "The Marmara Sea Section" is preferred rather than "the Marmara Region" or "the Marmara Section" only so as to prevent the connotation of the geographical region symbolized with the piece of land. The earthquake generation analysis was made according to the earthquakes with a minimum magnitude of 3. With this analysis, the magnitude-frequency relations of the sub-sections and the whole fault zone with various lengths, their annual average earthquake magnitudes ($\mathbf{M}_{ave.}$), their modal maximums ($\mathbf{Mod}_{max.}$), the greatest earthquake magnitudes likely to occur in a period of 100 years ($\mathbf{M}_{max.}^{100}$), their return periods for $\mathbf{M}_{max.}^{100}$ [$\mathbf{T}_d(\mathbf{M}_{max.}^{100})$], their return periods corresponding to magnitude 7.5 [$\mathbf{T}_d$(M = 7.5)] and their possible magnitudes corresponding to a return period of 250 years [$\mathbf{M}(T_d = 250)$] were computed according to two distinct investigation periods.

When Table 3 is considered, it is seen that the lowest seismic activity in the instrumental period (a= 2.780) occurred in the Central Black Sea Section; however, the level of activity for the whole zone was high but remained at the same level for the whole zone despite different zone lengths. It is observed that in the recent 38-year period, there was no low activity in the Central Black Sea Section (a= 4.869), although it was the minimum as compared with those of the other two sections, whereas the Marmara Sea Section displayed high activity (a= 5.402). For this period, the whole NAFZ displays higher seismic activity with no significant difference both with its sub-sections and as a whole notwithstanding different fault zone lengths as compared to the entire instrumental period. The difference between these two periods results from the improvement of earthquake observations. Even though the b- values show that everywhere along the whole zone has an identically high level of damage risk (b> -1.0), the risk turns out higher in the Karlıova Section as compared to the recent 38-year period (b= -1.025) and the Central Black Sea Section as compared to the 115-year period (b= -0.644). In Table 3, it is seen that different fault zone lengths are not significant concerning the matter for the overall trend. There is a high fit among all magnitude-frequency relations calculated ($|r| \geq 0.99$, Table 3). The greatest earthquake likely to occur in 100 years is calculated to be magnitude 8.4 at the most according to the data about the whole instrumental period, while it is calculated to be magnitude 7.6 at the most according to the data about the recent 38-year period (Table 3).

From the $\mathbf{M}_{ave.}$, $\mathbf{Mod}_{max.}$, $\mathbf{M}_{max.}^{100}$ and $\mathbf{T}_d(\mathbf{M}_{max.}^{100})$ values computed, it is seen that the NAFZ behaves similarly and even mostly the same according to the fault zone lengths of 1400 km, 1600 km and 2000 km (Table 3). Furthermore, Table 3 shows that the recurrence period of major earthquakes is shorter than 250 years for the NAFZ. The 250-year return period is computed for great earthquakes (Table 3). A mean displacement velocity of 2.2 cm/year corresponds to 227 years for an average slip of 5 m. This displacement velocity corresponds to an average slip of 4 m in 182 years.

The earthquake hazard analysis for the NAFZ was made according to the instrumental period (1900-2014), the period during which the national earthquake observation network reached a specific frequency (1977-2014), the sections of the related zone that can be separated from each other depending on the seismic activity character of the related zone (the Marmara Sea, Central Black Sea, and Karlıova) and its 2 characteristic branches in the Marmara Sea Section. Of the branches concerned, the northern branch in the Marmara Sea Section was referred to as northern strand and the southern branch as southern strand, while the area of the Zone between Marmara and Karlıova was referred to as the Anatolian Strand of NAFZ. Figure 9 shows the branches of the NAFZ in the Marmara Sea Section and the distributions of epicenters. In order not to further complicate the figure, the detail of NAFZ in the Marmara Region was not shown in Figure 6. Figure 9 contains some 5865 earthquakes with a minimum magnitude of 3.0 that occurred between 11/24/0029 and 12/31/2014. Of them, 5303 have a magnitude smaller than 4.0, while 562 are earthquakes with a magnitude of 4.0 and greater. The results of the earthquake hazard analysis made for the northern strand, southern strand, and the whole of NAFZ are provided in Table 4. As seen from Table 4, there is not any highly significant difference in earthquake frequency between the Marmara Sea Section and the branches (Table 3). However, although the southern strand appeared stiller than the northern strand in the instrumental period, the opposite was the case in the 1977-2014 period and the southern strand appeared more active and its damage risk appeared significantly low as compared to that of the northern strand. When the whole of NAFZ is compared with all the results for the NAFZ, it is understood that it displayed almost the same character. Hence, under the present available data resolution, there is no significant difference in seismic activity, character and hazard analysis between the whole NAFZ (for 1400, 1600, 2000 kms) and its branches. This might change when the appropriate data are accessed. For this purpose, new time and new studies are needed.

When the fault plane solutions in Figure 6 are considered, it is seen that they display a dominant strike-slip fault mechanism – which is the character of the NAFZ – with an orientation fitting the route of NAFZ's extension. Besides, again within the zone, it is sometimes possible to see some different mechanisms that are caused by both the Bitlis-Zagros thrust belt and the local differences stemming from either earth heterogeneity or geological formation rheology and that do not fit the character concerned. Additionally, the behaviors in areas under the influence of the Karlıova triple junction and the East Anatolian Fault Zone can be included in this.

Table 3. The seismicity analysis of North Anatolian Fault Zone. The data used is from the electronic earthquake catalogue of Boğaziçi University Kandilli Observatory and Earthquake Research Institute.

Investigation Period	**1900-2014** (115 years)						**1977-2014** (38 years)					
Explanation	The Marmara Sea Section	The Central Black Sea Section	Karlıova Section	The whole of NAFZ ΣL= 1400 kms	The whole of NAFZ ΣL= 1600 kms	The whole of NAFZ ΣL= 2000 kms	The Marmara Sea Section	The Central Black Sea Section	Karlıova Section	The whole of NAFZ ΣL= 1400 kms	The whole of NAFZ ΣL= 1600 kms	The whole of NAFZ ΣL= 2000 kms
Longitude Range *(° E)*	24-32	32-37.3	37.3-42.5	26-42.5	24-42.5	24-45.39	24-32	32-37.3	37.3-42.5	26-42.5	24-42.5	24-45.39
Range of M_c (M_{c1}-M_{c2})	3.0-6.5	3.7-6.4	3.4-7.9	3.6-7.9	3.4-6.5	3.5-6.5	3.0-6.0	3.3-6.0	3.3-6.4	3.0-6.4	3.0-6.1	3.0-6.2
Number of Data	6756	1541	3305	9658	11574	13919	6138	1441	3156	9010	10706	13004
a- value	4.137	2.780	3.417	3.799	4.062	4.117	5.402	4.869	4.936	5.537	5.649	5.742
δa	*0.01*	*0.00*	*0.01*	*0.02*	*0.00*	*0.01*	*0.01*	*0.02*	*0.02*	*0.01*	*0.01*	*0.01*
b- value	-0.829	-0.644	-0.727	-0.714	-0.754	-0.759	-1.084	-1.112	-1.025	-1.069	-1.078	-1.083
δb *($\times 10^{-1}$)*	*0.01*	*0.06*	*0.04*	*0.02*	*0.02*	*0.01*	*0.04*	*0.05*	*0.01*	*0.04*	*0.01*	*0.00*
σ	0.06	0.03	0.08	0.11	0.03	0.03	0.07	0.12	0.08	0.07	0.05	0.05
r	-1.00	-1.00	-1.00	-0.99	-1.00	-1.00	-1.00	-1.00	-1.00	-1.00	-1.00	-1.00
$\mathbf{M_{ave.}}$	4.5	4.2	4.5	4.4	4.4	4.4	4.6	4.2	4.5	4.8	4.8	4.8
$\mathbf{Mod_{max.}}$	4.4	4.1	4.3	4.9	5.0	5.0	4.5	4.0	4.6	4.8	4.9	4.9
$\mathbf{M_{max.}^{100}}$	7.9	7.5	7.5	8.2	8.3	8.4	7.4	6.4	6.7	7.4	7.5	7.6
$\mathbf{T_d}(M_{max.}^{100})$ *(year)*	97	98	108	97	95	99	95	111	108	98	96	106
$\mathbf{T_d}(M=7.5)$ *(year)*	57	98	108	37	32	30	111	947	637	117	96	89
$\mathbf{M}(T_d=250)$	8.6	8.2	8.1	8.9	9.0	9.1	8.0	6.8	7.1	7.9	8.0	8.1

***δa*, *δb*:** *Standard errors*
σ : Standard deviation
L: Elementary fault length
r : Correlation coefficient

$\mathbf{M_{ave.}}$**:** The average magnitude of the annually greatest earthquakes
$\mathbf{Mod_{max.}}$**:** Modal maximum
$\mathbf{M_{max.}^{100}}$ **:** Probable maximum magnitude for 100 years
$\mathbf{T_d}(M_{max.}^{100})$**:** Return period for $\mathbf{M_{max.}^{100}}$

$\mathbf{T_d}(M=7.5)$ **:** Return period versus magnitude 7.5
$\mathbf{M}(T_d=250)$**:** Probable magnitude correspond of the return period of 250 years
$\mathbf{M_c}$**:** The magnitude of completeness

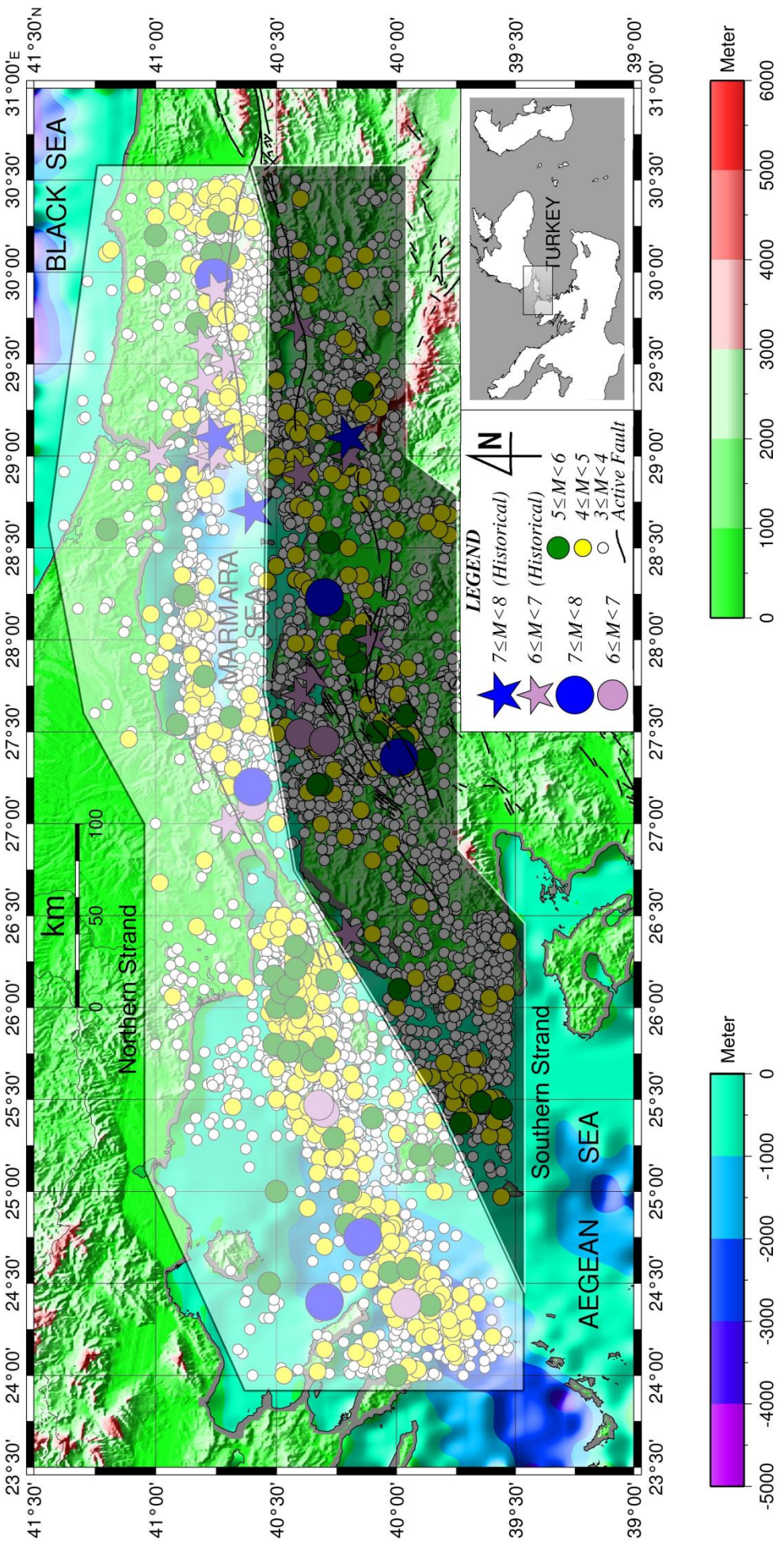

Figure 9. The major Western Segments of North Anatolian Fault Zone and their epicenter map. The map is based to 5865 earthquakes with magnitude of 3 and greater in the period 0029/11/24 - 2014/12/31. S - 1 and S - 2 are the northern and southern segments of the zone, respectively. Data is from the electronic earthquake catalogue of Boğaziçi University Kandilli Observatory and Earthquake Research Institute. Active faults on the map were to be put in order from Şaroğlu et al. (1992), and McClusky et al. (2000, 2003). The map was generated using GMT [61].

Table 4. The seismicity analysis for the major segments of North Anatolian Fault Zone. The data used is from the electronic earthquake catalogue of Boğaziçi University Kandilli Observatory and Earthquake Research Institute.

Investigation Period	1900 - 2014 (115 years)			1977 - 2014 (38 years)		
Branch	**Northern Strand**	**Southern Strand**	**Anatolian Strand**	**Northern Strand**	**Southern Strand**	**Anatolian Strand**
Longitude Range *(° E)*	24-30.5	24.95-30.5	30.5-41	24-30.5	24.95-30.5	30.5-41
Range of M_c (M_{c1}-M_{c2})	3.0-6.3	3.0-6.4	3.7-7.9	3.0-6.1	3.0-5.8	3.0-6.4
Number of Data	3594	2405	5219	3285	2117	4947
a- value	4.065	3.614	3.359	4.986	5.202	5.229
δa	*0.01*	*0.02*	*0.01*	*0.02*	*0.02*	*0.01*
b- value	-0.878	-0.824	-0.665	-1.045	-1.201	-1.036
δb ($\times 10^{-4}$)	*0.00*	*0.06*	*0.05*	*0.05*	*0.04*	*0.08*
σ	0.05	0.09	0.08	0.10	0.10	0.07
r	-1.00	-0.99	-1.00	-1.00	-0.99	-1.00
$M_{ave.}$	3.7	4.2	4.5	4.7	4.2	4.5
$Mod_{max.}$	4.0	3.9	4.6	4.4	4.1	4.6
$M_{max.}^{100}$	7.4	7.1	8.1	7.5	6.2	7.4
$T_d(M_{max.}^{100})$ *(year)*	106	95	96	103	108	94
$T_d(M=7.5)$ *(year)*	122	168	44	103	1920	111
$M(T_d=250)$	8.0	7.8	8.8	8.1	6.6	8.0

δa, δb: Standard errors
σ: Standard deviation
r : Correlation coefficient
$M_{ave.}$**:** The average magnitude of the annually greatest earthquakes
$Mod_{max.}$**:** Modal maximum
M_c**:** The magnitude of completeness
$M_{max.}^{100}$**:** Probable maximum magnitude for 100 years
$T_d(M_{max.}^{100})$ **:** Return period for $M_{max.}^{100}$
$T_d(M=7.5)$ **:** Return period versus magnitude 7.5
$M(T_d=250)$**:** Probable magnitude correspond of the return period of 250 years

VI. DISCUSSION

This study consists of two sections. One of them estimates new empirical relations for the NAFZ, follows its change, and estimates some kinematic parameters, while the other section investigates the recent condition of the seismicity of the zone concerned. The results in the first section are based on the data obtained from different reliable sources (Table 1) and obtained from the software specifically prepared for this study. There has not been any institution that exclusively observes and prepares such data for the NAFZ in the world yet. In other words, a national or an international institution that has estimated the earthquake parameters of all the earthquakes which occurred in this zone by using the latest technological possibilities and then optimized them and that then accurately made the other macroseismic observations in Table 1 has not existed yet. This does not

apply only to the NAFZ. This applies to every geographical region in the world, for which seismological and macroseismic data of at least 30 years are required. There are projects based on 3- to 5-year periods of observations made in Turkey in recent years. They monitor and examine known seismotectonic sources by high-resolution observation networks. It is probable that one day these studies will include the NAFZ in their scope too. Nevertheless, time and, from now on, a long observation period are needed to this end. Then, when evaluated with a realistic view and in terms of feasibility, these data do not have any alternatives for today either. Provided that it is considered from now on, some improvement might be achieved, but it will only be achieved with respect to the earthquake parameters and it will, and even has to, remain limited.

The displacement velocity estimated is an average value for the NAFZ and, with this feature, represents everywhere in the zone concerned. This is owing to the nature of the data used (Table 1). The data concerned are special for the approach used in this study when estimating displacement velocity and stress drop and have a unique value, and have included macroseismic observations. In other words, macroseismic parameters such as fault length (L) and the greatest relative displacement (U_m) are parameters that can only be measured in the macroseismic observation process following the earthquake concerned and they belong to the period and teams unique to that earthquake in the case of each earthquake. That is, if it is desired to measure the parameters concerned as macroseismic parameters each, this must be performed on the days immediately after the earthquake. Otherwise, they can of course be estimated more accurately from the seismogram. Each earthquake will certainly be studied by the appropriate teams in terms of its above-mentioned characteristics on the days following the coseismic process and the products will be duly shared. In this sense, the fact that the data are a compilation is therefore suitable for the quality of the related section of the study. Furthermore, they have no alternative anywhere in the world for today and for this zone. For instance, the fault length is either measured as the surface fault at that time or estimated from the seismogram. Today, it is impossible to re-perform a more accurate measurement for that earthquake or improve it. Thus, regardless of with which of the methods mentioned here this parameter is determined, it can be used by making a reference to the study concerned. Absolutely, this cannot be called a compilation.

The section, in which the current condition of seismicity is investigated, contains the data of the national observation network belonging to the institution explained in the related part of the study. As required by the above-mentioned explanations, if one intends to investigate this zone and its seismicity, these national data must be used. For today, the institution is the first address that one can refer to concerning these issues considering its experience, institutional adaptation to new developments, richness of archives, etc.

If we compare the 115-year data with the 38-year data for the whole NAFZ (Tables 3 and 4), we see that the results for the 38-year data describe a zone which is seismically more active and has a lower seismic risk in terms of the a- and b- values than those for the 115-year data (Table 3). Nevertheless, this lowness is some relative lowness. The absolute value of the b- value is also below 1 according to the 38-year data. The seismic activity turned out higher, which is concerned with the fact that this period of the earthquake catalogue is more orderly. This interpretation also applies to the segments of the NAFZ (Table 3). If we go on this comparison considering the earthquake likely to be encountered in the future and the recurrence period, the greatest earthquake likely to occur in 100 years turns out relatively smaller according to the 38-year data and this value is around magnitude 7.5 (Table 3). If we compare in terms of the period corresponding to magnitude 7.5, it is around 100 years according to the 38-year data but below 50 years according to the other one (Table 3). Therefore, the result for the 38-year data is more significant. If we consider the value of this period according to the segments of the NAFZ, the Marmara Sea Section appears closer to a possible earthquake with magnitude 7.5 in both periods. The reason for the high values seen in the 38-year data regarding this period is that the 38-year data contain a lower rate of major earthquakes than the 115-year data. Apart from them, if we also compare the two periods concerned in terms of a possible earthquake with a return period of 250 years, it is seen that magnitude values close to 8 are encountered according to the 38-year data, while magnitude values far above 8 and even close to 9 are estimated according to the other one (Table 3). From this, it turns out that the result for the 38-year data is more significant owing to the reality that the Zone has never generated any earthquake close to magnitude 9 so far. After all these interpretations, it might be stated that if used consciously, the recent 38-year data period (1977-2014) is a more preferable Turkish Earthquake Catalogue period for such analyses.

At this point, it can also be commented that depending on the calculations performed, the greatest earthquake likely to occur in 100 years is around magnitude 8 for the whole Zone (Tables 3 and 4). On the other hand, the greatest earthquake likely to occur in the Zone in 250 years is found to be around magnitude 8.5 (Tables 3 and 4). Besides, the return period for magnitude 7.5 is at the level of 100 years. However, we look at the available earthquake catalogue and no earthquake greater than magnitude 8 has occurred in this Zone so far. This means that the magnitudes around 8.5, found for 250 years, are not very significant! That is, it seems that earthquakes of this size have not been accessed very much. Given this, the recurrence period of a major earthquake in this Zone is most probably below 250, and even 200, years according to the Seismological classification because when the duration is 250 years, the magnitude shoots up to the level of 8.5. In real life, however, we do not encounter such a magnitude level when we consider all the earthquakes that have occurred so far.

Furthermore, from the evaluations made according to both periods, it is interpreted that the southern strand of the NAFZ has high seismic activity as well as a seismic risk which is in harmony with the whole Zone. Here it becomes important that the earthquake catalogue should be used consciously together with the period addressed because when the values of the 38-year data in Table 4 are considered, it is seen that the southern strand of the NAFZ appears as if earthquakes would not occur very much. Nevertheless, this absolute meaning is incorrect. Hence, if the origin of the data and its place in the whole process are included consciously in the evaluation when evaluating the results, that absolute meaning turns out to be an apparent meaning only.

When the GPS (the Global Positioning System) measurements are considered, it is seen that the values of slip rate provided for the Marmara Region by Doğan et al. (2006, 2003) are around 20 mm/year. Figure 10 shows the slip rates of the Marmara Region. The velocities in Figure 10 generally vary around this value and around ± 3 mm/year. With a GPS study by Yavaşoğlu et al. (2005, 2011), it is seen that the general character of the slip rate vectors in the central Anatolia section of the NAF varies around 20 mm/year. This value is approximately ± 3 mm/year in the zone. Figure 11 shows the velocity vectors in the central Anatolia section of the NAFZ according to the Eurasian Plate. Although the slip rate vectors vary up to 24 mm/year according to the GPS observations in the eastern section of the NAFZ by Özener et al. (2005), the error ellipses are great in most of them. Figure 12 shows the slip rate vectors of the eastern section of the NAFZ. These values will become more stable as the number of observations increases and resolution is enhanced. The slip rate fields derived by Reilinger et al. (2006) range from 24.2 to 28.0 mm/year along northern strand in this study, while they range from 24.2 to 25.8 mm/year in the eastern half of the NAFZ. Figures 13 and 14 show the fault plane slip rates for the western and eastern halves of the NAFZ, respectively. The significantly low velocities in the southern branch of the NAFZ in Figure 13 can be interpreted as an indication of the fact that the northern branch is more dominant today. Moreover, the southern branch is also under the influence of the Aegean extensional system and it is therefore the meeting point of two different tectonic systems. However, it should be borne in mind that the figures evaluated are derived values. Nevertheless, when the values in Figure 10 are considered, a noteworthy difference is not overlooked. At this point, tectonic reality, the characteristic of being derived values and the difference with the GPS observations tell something: more time and a continuous observation of quality are needed to talk about these accessed values in a more binding fashion. Observations with such features have been launched in recent years. Unless there is an unexpected interruption, time is the only problem. Moreover, the recent studies performed by Sunal et al. (2012) and Turk et al. (2012) have presented similar results.

The value estimated with the GPS observations is compatible and significant. In time, resolution will be enhanced with an increase in the GPS observation points and one day it will be possible to know the slip rate with ranges in meters. This is only possible through a significant increase in the number of observations and their continuity.

Owing to the scope of the available data, it is impossible to calculate individual stress drops for the branches defined (northern strand, southern strand, and the whole of NAFZ) (Table 1). To overcome this, a new period with earthquakes that form surface faults is needed. In other words, the scope of the available data has to extend both in time and space. As also seen from Equation (10), the approach used in this study for stress drop is sensitive to fault geometry. Fault geometry is defined as a rectangular fault plane. Thus, this approach is not sensitive to any geometric parameter other than the geometric parameters mentioned in Equation (10). To access more information than this point, the geometric parameters concerned should be well estimated or observed in new earthquakes with new approaches.

VII. CONCLUSION and EVALUATION

The seismological analysis made according to 29 earthquakes with minimum magnitude 4.8 (m_b, M_s) that occurred in the North Anatolian Fault Zone in the 1909-2000 period and the macroseismic and instrumental observations of which were made is the latest seismological identity of the NAFZ. Accordingly, no change in character other than the numerical difference is observed in the seismic moment-magnitude relations and stress drop changes, whereas slightly different results are obtained for seismic moment-fault plane relation and the mean displacement velocity. For the NAFZ, the *optimum* mean displacement velocity is 2.2 cm/year, and the possible threshold magnitude of the earthquakes that might form a visible surface fault is computed as 6.2 (M_s).

According to the values of stress drop obtained from the calculations wherein the zone length and the focal depth are considered 1400 km and 15 km, respectively, it is seen that the highest stress drops correspond to the area between Çanakkale and Balıkesir, the surroundings of İzmit, Sakarya and Bolu, the area between Kastamonu and Bartın, the area among Samsun, Amasya and Tokat, and the area among Erzincan, Karlıova and Tunceli. Particularly the section of the NAFZ to the east of Bolu, its section between Amasya and Kastamonu, its section around the triangle of Sivas, Ordu and Giresun and the surroundings of Erzurum, Bingöl and Muş, where there is no stress drop, may be interpreted as the places in which the process of storage of the strain energy has not ended. Also from Figure 5, it is seen that the stress accumulation has not been released in the Marmara Sea yet. This region is the first-ranking place as a candidate for the expectation of a possible major earthquake that might occur in Turkey in the future or perhaps in some not too distant time. However, this reality is not the reason for the absurd interpretation that the earthquakes in the

NAFZ migrate westwards, for the development of earthquakes from both (sides) ends of the faults and of the fault zones will continue. This is a geological and tectonic rule. That is to say, the earthquake hazard in the east of the NAFZ or of its segments is at least as much as

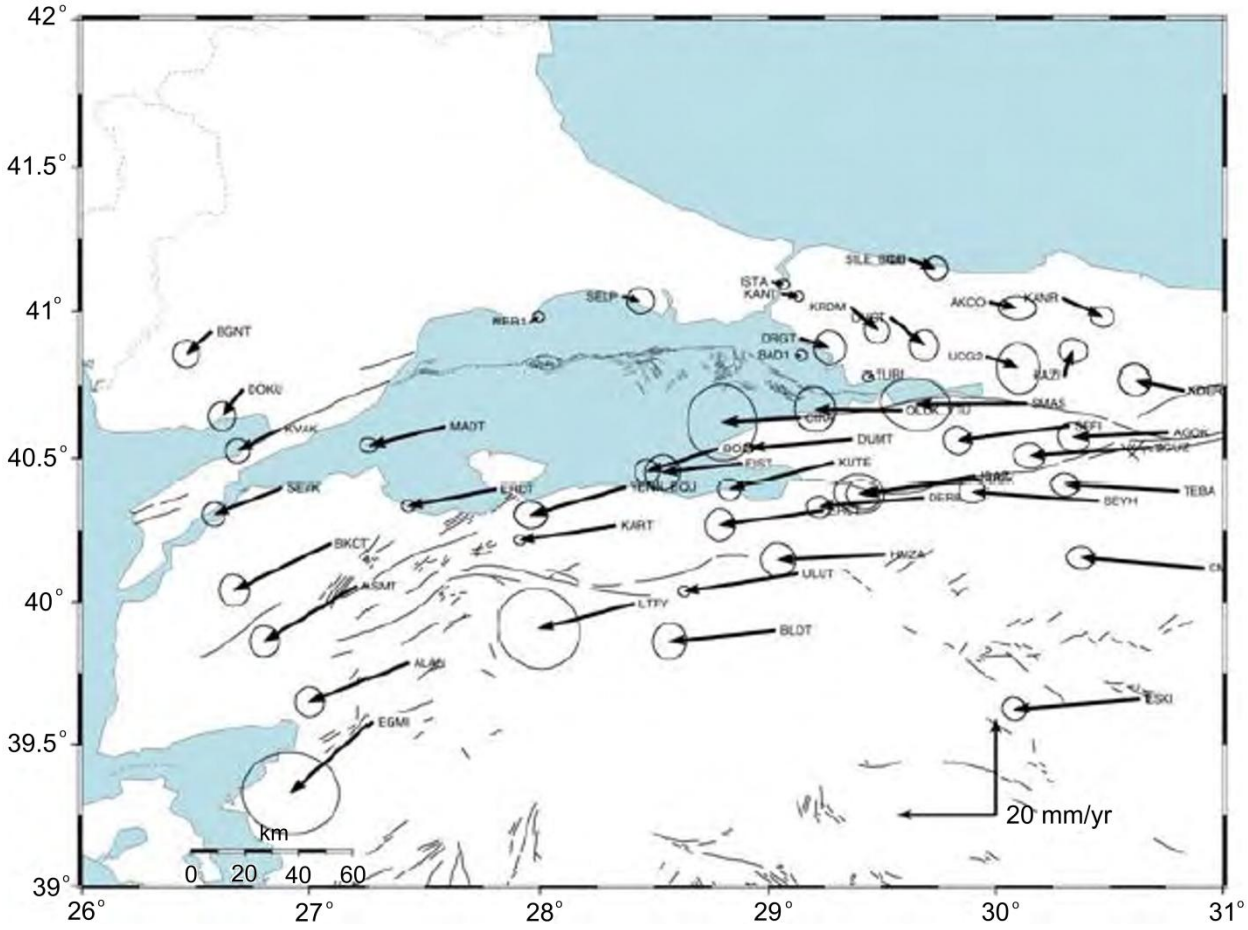

Figure 10. Horizontal slip rate field of the Marmara Region in a Eurasian fixed frame [18].

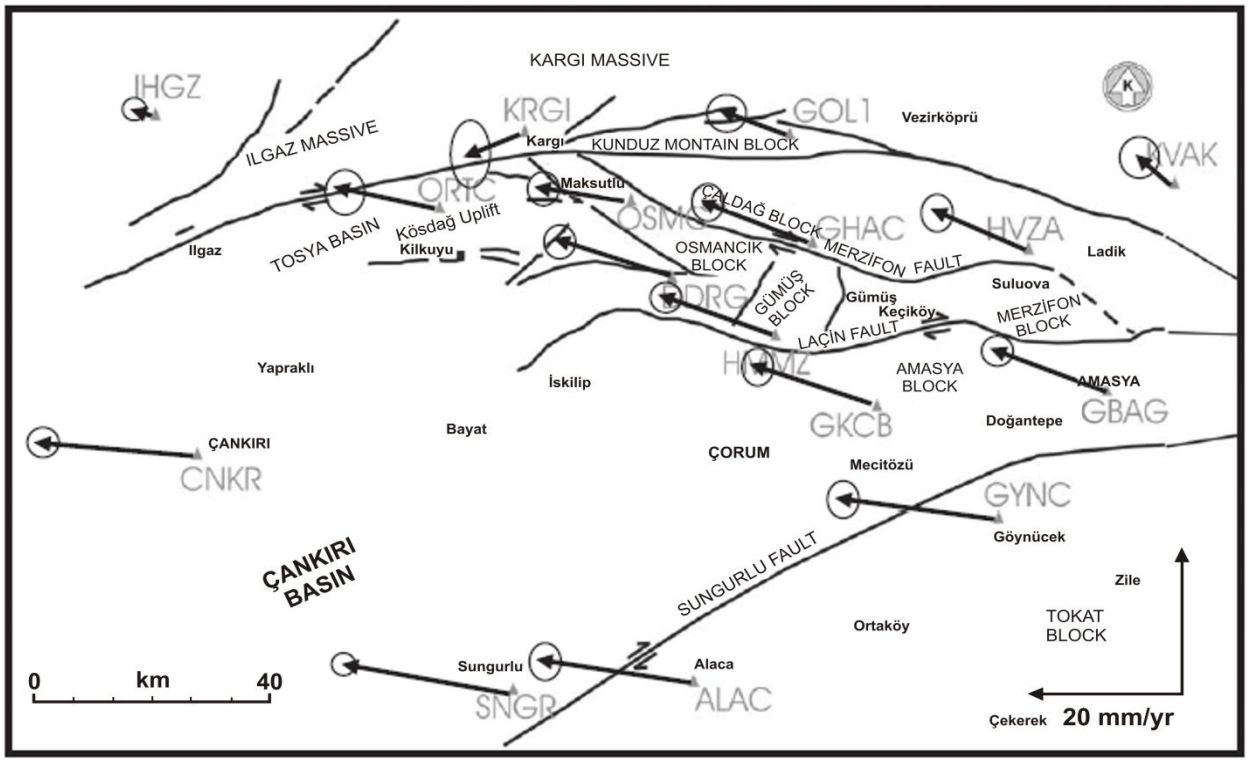

Figure 11. Slip rate vectors of the Middle-Anatolian Part of North Anatolian Fault Zone in a Eurasian fixed frame [63].

that in its west. Nevertheless, the risk is different. Although the Marmara Region is also striking in Figure 5, it should be considered that the strain accumulation is being released with activities such as the August 17, 1999 (M_w=7.4) Kocaeli-Gölcük earthquake and particularly the September 21, 1999 (M_d=5.0) earthquake in the Marmara Sea that occurred in the offshore part of Tekirdağ in the following process. The following should be added to the comment above: we can add the Kastamonu-Çankırı-Çorum-Amasya-Samsun-Sinop quadrangle and the place between Tokat and Gümüşhane (naturally, Sivas-Tunceli-Giresun-Ordu will be affected by this too!) as well as the Bingöl-Muş-Erzurum-Bayburt quadrangle to the Marmara Sea and its close vicinity as the first-ranking candidate places for the expectation of an earthquake. The stress accumulation of the zone concerned and the rheology of the formation in the areas concerned will determine their order of precedence.

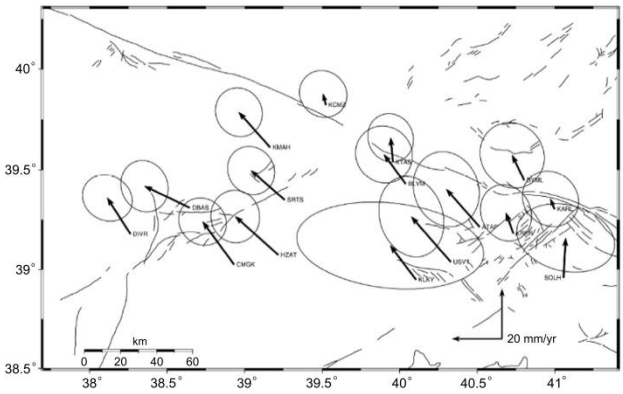

Figure 12. Slip rate vectors of the Eastern Part of North Anatolian Fault Zone in a Eurasian fixed frame [42].

The return period of a possible major earthquake to be generated by this zone is 250 years at the most. In other words, an earthquake like the August 17, 1999 (M_w=7.4) earthquake will occur once every 100 years on average. The a- and b- values that characterize the Zone are 4 and -0.8, respectively. The average magnitude of the annually greatest earthquakes is 4.5. The modal maximum is 4.5 as well.

When the obtained results are compared with the results known from previous studies, it appears that the results accessed within the scope of this study are more reliable both in terms of the length of the process considered in this study and the quality of the data used. Given this, when the behaviors of the NAFZ are monitored, it is seen that some seismological characters (such as seismic moment-magnitude relation, the change in stress drop, and threshold magnitude) remained stable, whereas some of them (such as seismic moment-fault plane relation and the mean slip rate) changed. Furthermore, it is useful to make studies that will provide a more accurate ground for the information about focal depths along the NAFZ. Beyond this, new, high-resolution and multidisciplinary observation networks that well cover the Zone and the continuity of which has been ensured are needed. For this purpose, it is necessary to establish a new observation-evaluation system with additional teams and equipment

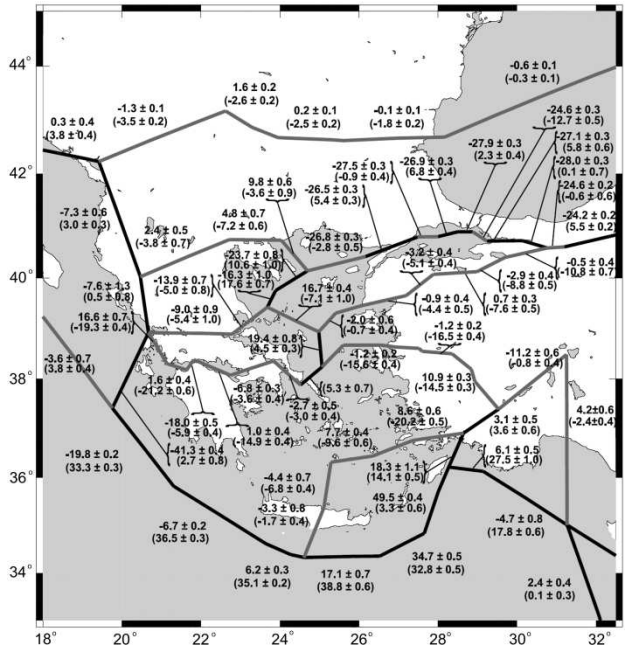

Figure 13. Fault slip rates (mm/yr) belong to the Western Part of North Anatolian Fault Zone deduced by the block modelling [45]. Top numbers (no parentheses) are strike-slip rates, positive being left-lateral. Numbers in parentheses are fault-normal slip rates, positive being closing.

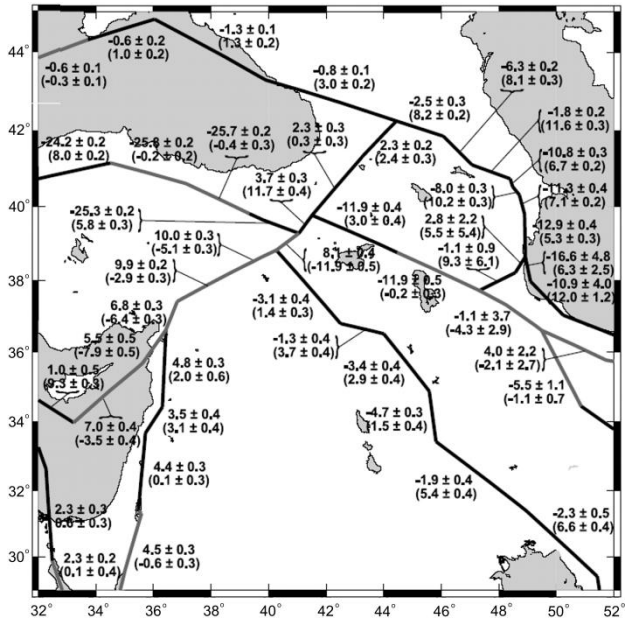

Figure 14. Fault slip rates (mm/yr) belong to the Eastern Part of North Anatolian Fault Zone deduced by the block modelling [45]. Top numbers (no parentheses) are strike-slip rates, positive being left-lateral. Numbers in parentheses are fault-normal slip rates, positive being closing.

according to a new work plan also by utilizing those that are available. The reason why no distinct hazard analysis can be made for the middle branch of the NAFZ in the

Marmara region is that the border separating this branch from the southern strand cannot be determined soundly either in terms of the epicenter distribution or in the tectonic sense. If this tectonic border can be determined digitally with some fieldwork, an opportunity will be created to make the analysis concerned accurately and this will also be useful for future studies.

ACKNOWLEDGEMENT

The author thanks Kandilli Observatory and Earthquake Research Institute of Boğaziçi University, which keeps the earthquake data open for researchers' use, and Harvard University, which performed the CMT solutions, for their all labor.

REFERENCES

[1] Aki K, Richards, PG (1980). Quantitative Seismology Theory and Methods. Vol. I, Vol. II., 932 p, USA: W.H. Freeman and Co., San Francisco.

[2] Aki K (1972). Earthquake mechanism. Tectonophysics, 13: 423 - 446.

[3] Ambraseys NN, Jackson JA (2000). Seismicity of the Sea of Marmara (Turkey) since 1500. Geophys. J. Int., 141: F1 - F6.

[4] Ambraseys NN (1970). Some characteristic features of the Anatolian Fault Zone. Tectonophysics, 9: 143 - 165.

[5] Barka A, Akyüz S, Altunel E, Sunal G, Çakır Z, Dikbaş A, Yerli B, Rockwell T, Dolan J, Hartleb R et al. (2000). The August 17, 1999 İzmit earthquake, M = 7.4, Eastern Marmara region: Study of surface rupture and slip distribution. In: Barka A, Kozacı Ö, Akyüz S, Altunel E (eds), İzmit and Düzce Earthquakes: preliminary results, İstanbul Technical University Press, İstanbul, pp. 15 - 30.

[6] Barka A (1996). Slip distribution along the North Anatolian Fault associated with the large earthquakes of the period 1939 to 1967. Bull.Seismol.Soc.Am., 86: 1238 - 1254.

[7] Barka A (1992). The North Anatolian Fault Zone. Annales Tectonicae, 6(supplement): 164 - 195.

[8] Barka A, Kadinsky-Cade K (1988). Strike-slip fault geometry in Turkey and its influence on earthquake activity. Tectonics, 7: 663-684.

[9] Bayrak Y, Öztürk S (2004). Spatial and temporal variations of the aftershock sequences of the 1999 İzmit and Düzce earthquakes. Earth P. Space, 56: 933 - 944.

[10] Bayrak Y , Çınar H , Bayrak E (2011). "The North Anatolian Fault Zone: an Evaluation of Earthquake Hazard Parameters", New Frontiers in Tectonic Research - At the Midst of Plate Convergence, Uri Schattner (Ed.), ISBN: 978-953-307-594-5, InTech, Available from: http://www.intechopen.com/articles/show/title/the-north-anatolian-fault-zone-an-evaluation-of-earthquake-hazard-parameters.

[11] Brune JN (1968). Seismic moment, seismicity and rate of slip along major fault zones. J.Geophys.Res., 73: 777 - 784.

[12] Brune JN, Allen CR (1967). A low stress-drop, low magnitude earthquake with surface faulting: The Imperial, California earthquake of March 4, 1966. Bull.Seismol.Soc.Am., 57: 501 - 514.

[13] Canıtez N, Ezen Ü (1973). Slip rate and stress-drop along the North Anatolian Fault Zone. Symposium on Earthquake Statistic and Risk, Unesco Balkan Project, İstanbul (unpubl.).

[14] Canıtez N, İlkışık M (1973). Statik Dislokasyon Alanları Üzerine Deprem Odağının Geometrisinin Etkisi (Affect of Earthquake Focus Geometry on the Static Dislocation Fields). Turkish Council of Scientific and Technology, Project of Engineering Investigation Group, No. MAG - 292, Ankara, Turkey.

[15] Castellaro S, Mulargia F, Kagan YY (2006). Regression problems for magnitudes. Geophys J. Int. 165: 913–930.

[16] Delouis B, Giardini D, Lundgren P, Salichon J (2002). Joint inversion of InSAR, GPS, teleseismic, and strong-motion data for the spatial and temporal distribution of earthquake slip: application to the 1999 İzmit mainshock. Bull.Seismol.Soc.Am., 92: 278 - 299.

[17] Dewey JW (1976). Seismicity of Northern Anatolia. Bull. Seismol. Soc. Am., 66: 843 - 868.

[18] Doğan U, Demirel H, Aydın C, Ergintav S, Çakmak R, Belgen A, Gerstenecker C (2006). GPS and Gravity Measurements along the Western Part of the North Anatolian Fault and their relation to Crustal Deformations. 1st International Symposium of the International Gravity Field Service, Gravity Field of the Earth, August 28 - September 01, 2006, İstanbul, (Journal of Harita, No. 18, Special Issue, Turkey).

[19] Doğan U, Ergintav S, Demirel H, Çakmak R, Özener H (2003). Estimation of the time-dependent crustal movements of the İzmit Earthquake. J. of Geodyn., December 2003, 36: 615 - 632.

[20] Eyidoğan H, Güçlü U, Utku Z, Değirmenci E (1991). Türkiye Büyük Depremleri Makro - Sismik Rehberi (1900 - 1988) [Macro - seismic Catalogue of Major Turkish Earthquakes between 1900 - 1988]. Istanbul Technical University, Faculty of Mines, Department of Geophysical Engineering, Istanbul, Turkey.

[21] Ezen Ü (1981). Earthquake-source parameters related to magnitude along the North Anatolian Fault Zone. Bullet. of IISEE, 19: 33 - 55.

[22] Ezen Ü, Irmak TS (2007). The Stres Drops in the North Anatolian Fault (Turkey) Zone During the 1939 - 1999. International Earthquake Symposium - Kocaeli 2007, Turkey, Web pp. 152 - 161 (http://kocaeli2007.kocaeli.edu.tr/kocaeli2007/152-161.pdf), October 22 - 24, 2007, Kocaeli,Turkey.

[23] Galanopoulos AG (1965). The large conjugate fault system and the associated earthquake activity in Greece. Ann. Geol. Pays Hellen, 18: 119 - 134.

[24] Gumbel EJ (1958). Statistics of extremes. Columbia University Press, New York.

[25] Gutenberg B, Richter CF (1944). Frequency of earthquakes in California. Bull. Seismol. Soc. Am., 34: 185 - 188.

[26] Gutenberg B, Richter CF (1942). Earthquake magnitude, intensity, energy and acceleration. Bull. Seismol. Soc. Am., 32: 163 - 191.

[27] Gülen L, Pınar A, Kalafat D, Özel N, Horasan G, Yılmazer M, Işıkara AM (2002). Surface fault breaks, aftershock distribution, and rupture process of the 17 August 1999 İzmit, Turkey, earthquake. Bull. Seismol. Soc. Am., 92: 230 - 244.

[28] Gürbüz C, Aktar M, Eyidoğan H, Cisternas HP, Haessler H, Barka A, Ergin M, Türkelli N, Polat O, Üçer SB et al. (2000). The seismotectonics of the Marmara region (Turkey): results from a microseismic experiment. Tectonophysics, 316: 1 - 17.

[29] Kalafat D, Kekovalı K, Güneş Y, Yılmazer M, Kara M, Deniz P, Berberoğlu M (2009). Türkiye ve Çevresi Faylanma-Kaynak Parametreleri (MT) Kataloğu (1938-2008) [A Catalogue of Source Parameters of Moderate and Strong Earthquakes for Turkey and its Surrounding Area (1938-2008)]. Boğaziçi Üniversitesi, Kandilli Rasathanesi ve Deprem Araştırma Enstitüsü, İstanbul, ISBN 978 – 975 – 518 – 303 – 9.

[30] Kijko A, Sellevoll MA (1992). Estimation of earthquake hazard parameters from incomplete data files, Part II: Incorporation of magnitude heterogeneity. Bull. Seismol. Soc. Am., 82: 120-134.

[31] Kijko A, Sellevoll MA (1989). Estimation of earthquake hazard parameters from incomplete data files. Part I. Utilization of extreme and complete catalogs with different threshold magnitudes. Bull. Seismol. Soc. Am., 79: 645-654.

[32] Konstantinou KI (2014). Moment Magnitude–Rupture Area Scaling and Stress-Drop Variations for Earthquakes in the Mediterranean Region. Bull. Seismol. Soc. Am., 104: 2378–2386, doi: 10.1785/0120140062.

[33] McClusky S, Reilinger R, Mahmoud S, Ben Sari D, Tealeb A (2003). GPS constraints on Africa (Nubia) and Arabia plate motions. Geophys. J. Int., 155: 126 – 138.

[34] McClusky S, Balssanian S, Barka A, Demir C, Ergintav S, Georgiev I, Gurkan O, Hamburger M, Hurst K, Kahle H et al. (2000). Global Positioning System constraints on plate

kinematics and dynamics in the eastern Mediterranean and Caucasus. J. Geophys. Res., 105: 5695 – 5719.

[35] McKenzie DP (1972). Active tectonics of the Mediterranean region. Geophys. J. R. Astr. Soc., 30: 109 - 185.

[36] McKenzie DP (1970). Plate tectonics of the Mediterranean region. Nature, 226: 239 - 243.

[37] Ketin İ (1969). Über die nordanatolische horizontal-verschiebung. Bull. Mineral. Res. Exploration Inst. Turkey, Foreign Ed., 72: 1 - 28.

[38] Ketin İ (1957). Kuzey Anadolu Deprem Fayı (North Anatolian Earthquake Fault). Journ. of İstanbul Technical University, 15: 49 - 52 (in Turkish), İstanbul, Turkey.

[39] Ketin İ, Roesli F (1953). Macroseismische untersuehungen über das nordwestanatolische Beben won 18 März 1953, Eclogae.Geol. Helvetiae, 46: 187 - 208.

[40] KOERI (Kandilli Observatory and Earthquake Research Institute) (2001). Boğaziçi University, İstanbul, Turkey.

[41] Le Pichon X, İmren C, Rangin C, Şengör AMC, Siyako M (2014). The South Marmara Fault. Int. J. Earth Sci. (Geol Rundsch), 103: 219-231, doi 10.1007/s00531-013-0950-0.

[42] Özener H, Doğru AG, Turgut B, Yılmaz O, Ergintav S, Çakmak R, Sanli U, Arpat E, Gülen L, Gürkan O (2005). Kuzey Anadolu Fayı Doğu Kesiminin Kabuk Deformasyonlarının ve Blok Kinematiğinin GPS Ölçme Tekniği İle Araştırılması (Investigation by using GPS Measurements of the Crustal Deformations and Block Kinematics in the Eastern Part of North Anatolian Fault Zone). 10th Surveying Scientific and Technical Congress of Turkey, Union of Chambers of Turkish Engineers and Architects, Chamber of Surveying Engineers, March 28 - April 1, 2005, Ankara, Turkey.

[43] Polat O, Eyidoğan H, Haessler H, Cisternas HP, Philip H (2002a). Analysis and interpretation of the aftershock sequence of the August 17, 1999, İzmit (Turkey) earthquake. J. of Seismol., 6: 287 - 306.

[44] Polat O, Haessler H, Cisternas HP, Eyidoğan H, Aktar M, Frogneux M, Comte D, Gürbüz C (2002b). The İzmit (Kocaeli), Turkey Earthquake of 17 August 1999: Previous Seismicity, Aftershocks, and Seismotectonics. Bull. Seismol. Soc. Am., 92: 361 - 375.

[45] Reilinger R, McClusky S, Vernant P, Lawrence S, Ergintav S, Cakmak R, Ozener H, Kadirov F, Guliev I, Stepanyan R et al. (2006). GPS constraints on continental deformation in the Africa-Arabia-Eurasia continental collision zone and implications for the dynamics of plate interactions. Journal of Geophysical Research, 111, no.B05411, doi:10.1029/2005JB004051.

[46] Senatorski P (2012). Effect of seismic moment–area scaling on apparent stress–seismic moment relationship. Phys. Earth Planet. Inter., 196–197: 14–22.

[47] Scholz CH (2002). The mechanics of earthquakes and faulting, 2nd Edition, Cambridge University Press, 471 p.

[48] Shaw BE (2013). Earthquake surface slip-length data is Fit by Constant Stress Drop and is Useful for Seismic Hazard Analysis. Bull. Seismol. Soc. Am., 103: 876–893, doi: 10.1785/0120110258.

[49] Shaw BE, Wesnousky S (2008). Slip-Length Scaling in Large earthquakes: The Role of Deep-Penetrating Slip below the Seismogenic Layer. Bull. Seismol. Soc. Am., 98: 1633–1641, doi: 10.1785/0120070191.

[50] Sunal G, Erturaç MK (2012). Estimation of the pre-North Anatolian Fault Zone pseudo-paleo-topography: A key to determining the cumulative offset of major post-collisional strike-slip faults. Geomorphology, 159-160: 125 - 141.

[51] Şaroğlu F, Emre Ö, Kuşçu İ (1992). Active Fault Map of Turkey. General Directorate of Mineral Research and Exploration, Ankara, Turkey.

[52] Şengör AMC, Grall C, İmren C, Le Pichon X, Görür N, Henry P, Karabulut H, Siyako M (2014). The geometry of the North Anatolian transform fault in the Sea of Marmara and its temporal evolution: implications for the development of intracontinental transform faults. Can. J. Earth Sci., 51: 222-242, dx.doi.org/10.1139/cjes-2013-0160.

[53] Şengör AMC, Tüysüz O, İmren C, Sakınç M, Eyidoğan H, Görür N, Le Pichon X, Rangin C (2005). The North Anatolian Fault: A new look. Annu. Rev. Earth Planet. Sci., 33: 37–112, doi: 10.1146/annurev.earth.32.101802.120415.

[54] Şengör AMC (1979). The North Anatolian Transform Fault: its age, offset and tectonic significance. J. Geol. Soc. London, 136: 269 - 282.

[55] Şengör AMC, Canıtez N (1982). The North Anatolian Fault, Alpine Mediterranean Geodynamics. AGU, Geodynamics Series, 7: 205 - 216.

[56] Toksöz MN, Shakal AF, Michael AJ (1979). Space - Time Migration of Earthquakes along the North Anatolian Fault Zone and Seismic Gaps. Pure and Applied Geophysics, 117: 1258 - 1270.

[57] Turk T, Gümüşay U, Tatar O, Sunal G, Erturaç MK (2012). Creating infrastructure for seismic microzonation by Geographical Information Systems (GIS): A case study in the North Anatolian Fault Zone (NAFZ). Computers and Geosciences, 43: 167 - 176.

[58] Utku M (2003). The Last Seismological Identify of the North Anatolian Fault System. International Workshop on the North Anatolian, East Anatolian and Dead Sea Fault Systems: Recent Progress in Tectonics and Paleoseismology, and Field Training Course in Paleoseismology, Abstracts, p.92, 31 August - 12 September 2003, Middle East Technical University (METU) Cultural and Convention Center, Ankara.

[59] Utsu T, Ogata Y, Matsu'ura RS (1995). The Centenary of the Omori Formula for a Decay Law of Aftershock Activity. J. Phys. Earth, 43: 1-33.

[60] Wells DL, Coppersmith KJ (1994). New Empirical Relationships among Magnitude, Rupture Length, Rupture Width, Rupture Area, and Surface Displacement. Bull.Seismol.Soc.Am., 84: 974 - 1002.

[61] Wessel P, Smith WHF (2006). The Generic Mapping Tools (GMT) version 4.1.4 Technical Reference & Cookbook, NOAA/NESDIS.

[62] Yamamoto Y, Takahashi N, Citak S, Kalafat D, Pinar A, Gurbuz, C, Kaneda Y (2015). Offshore seismicity in the western Marmara Sea, Turkey, revealed by ocean bottom observation. Earth, Planets and Space 67:147, DOI 10.1186/s40623-015-0325-9.

[63] Yavasoglu H, Tari E, Karaman H, Sahin M, Baykal O, Erden T, Bilgi S, Ruzgar G, Ince CD, Ergintav S et al. (2005). GPS Measurements along the North Anatolian Fault Zone on the Mid-Anatolia Segment, Geodetic Deformation Monitoring: From Geophysical to Engineering Roles International Association of Geodesy Symposia (IAG) Symposium Jaén, Spain, March 17 – 19, 2005, vol.131, Springer, ISSN0939 - 9585, ISBN978 – 3 – 540 – 38595 – 0 (Print) 978 – 3 – 540 – 38596 – 7 (Online).

[64] Yavaşoğlu H, Tari E, Tüysüz O, Çakir Z, Ergintav S (2011). Determining and modeling tectonic movements along the central part of the North Anatolian Fault (Turkey) using geodetic measurements. Journal of Geodynamics, 51: 339 - 343.

[65] Yucemen MS, Akkaya AD (2012). Robust estimation of magnitude-frequency relationship parameters. Structural Safety, 38: 32 - 39.